Supplementary Material: Quantifying the economic response to COVID-19 mitigations and death rates via forecasting Purchasing Managers' Indices using Generalised Network Autoregressive models with exogenous variables

Guy P. Nason and James L. Wei

Department of Mathematics, Huxley Building, Imperial College London, London, UK.

E-mail: g.nason@imperial.ac.uk, james.wei19@imperial.ac.uk

[Received 30 Nov 2020. Revised 2 Jun 2021]

Part 1: Models and Theory

1. The models of Zhu *et al.* (2017) and Knight *et al.* (2020)

For completeness the model from Zhu et al. (2017) is as follows. Let $Y_{i,t}$ be the response collected from the ith subject at time t, where $i = 1, \ldots, N$ and t is thought of as time. Each subject can be thought of as a node in a network and each node may have associated a p-dimensional node-specific random (covariate) vector $Z_i = (Z_{i,1}, \ldots, Z_{i,p})^\intercal$. Their network vector autoregression model (NAR) is given by

$$Y_{i,t} = \beta_0 + Z_i^\intercal \gamma + \beta_1 n_i^{-1} \sum_{j=1}^{N} a_{i,j} Y_{j,(t-1)} + \beta_2 Y_{i,(t-1)} + \epsilon_{i,t}, \tag{1}$$

where $n_i = \sum_{j \neq i} a_{i,j}$ is the total number of nodes that i follows, where $a_{i,j} = 1$ is there is a relationship (edge) between i and j and $a_{i,j} = 0$, otherwise, β_0 is a level effect parameter, β_1 is a network effect parameter, β_2 is the standard AR(1) parameter and γ is a p-dimensional covariate parameter.

The model of Knight et al. (2020) is

$$X_{i,t} = \sum_{j=1}^{p} \left(\alpha_{i,j} X_{i,t-j} + \sum_{c=1}^{C} \sum_{r=1}^{s_j} \beta_{j,r,c} \sum_{q \in \mathcal{N}^{(r)}(i)} \omega_{i,q,c} X_{q,t-j} \right) + u_{i,t}, \tag{2}$$

where the quantities here are the same as in the main paper except here there is an extra index c in the network part, which represents one of C possible different edge types (for example, in epidemics, $C = 2$ might arise because viruses might spread by wind (edge type $c = 1$) or by physical communication (edge type $c = 2$). This model was developed from the NARIMA model from Knight et al. (2016), which does not have edges types, but introduces differencing and a moving average component as is found in standard ARIMA modelling for time series, see, e.g. Priestley (1983), Brockwell and Davis (1991), Hamilton (1994) or Chatfield (2003).

2. Stationarity conditions for the GNARX model

THEOREM 2.1. *The GNARX model, as defined in (1) of the main report, is stationary under the conditions that the external regressor time series $\mathbf{X}_t$ are stationary and*

$$\sum_{j=1}^{p}\left(|\alpha_{i,j}|+\sum_{c=1}^{C}\sum_{r=1}^{s_j}|\beta_{j,r,c}|\right)<1 \quad \forall i\in 1,...,N. \tag{3}$$

The GNARX model can be expressed in VARX form as

$$\mathbf{Y}_t=\phi_1\mathbf{Y}_{t-1}+\cdots+\phi_p\mathbf{Y}_{t-p}+\Lambda_0\mathbf{X}_t+\Lambda_1\mathbf{X}_{t-1}+\cdots+\Lambda_{p'}\mathbf{X}_{t-p'}+\mathbf{u}_t, \tag{4}$$

where the coefficient matrices are restricted such that $\phi_k = \text{diag}\{\alpha_{i,k}\}+\sum_{r=1}^{s_k}\beta_{k,r}W^{(r)}$, $[W^{(r)}]_{l,m}=w_{l,m}\mathbb{I}\{m\in\mathcal{N}^{(r)}(l)\}$, and $\Lambda_k=\lambda_k I_N$. Equation 4 can be expressed compactly in terms of lag polynomials as

$$\phi(B)\mathbf{Y}_t=\Lambda(B)\mathbf{X}_t, \tag{5}$$

where $\phi(z)=I_n-\phi_1 z-...-\phi_p z^p$ and $\Lambda(z)=I_n-\Lambda_1 z-...-\Lambda_p z^p$. Knight et al. (2020) demonstrate that under Equation 3, the causality criterion $\det\phi(z)\neq 0$ for all $|z|\leq 1$, where $z\in\mathbb{C}$, is satisfied. By Brockwell et al. (1991), we can thus obtain the representation

$$\mathbf{Y}_t=\sum_{j=0}^{\infty}\psi_j\mathbf{X}_{t-j}, \tag{6}$$

where the coefficient matrices ψ_j correspond to the lag polynomial $\psi(z)=\phi^{-1}(z)\Lambda(z)$. As $\mathbf{X}_t$ are stationary by assumption, $\mathbf{Y}_t$ is therefore stationary.

3. Consistency and asymptotic normality of GNARX parameter estimates

A straightforward application of Lütkepohl (2005) Proposition 5.1, with an additional assumption that the external regressor time series are stationary, results in the following asymptotic properties of $\hat{\gamma}^{FGLS}$, which we provide without proof.

THEOREM 3.1. *Let $\hat{\gamma}^{FGLS}$ and $\hat{\Sigma}_u$ be defined according to (5) and (6) from the main paper, respectively, for stationary multivariate time series $\{\boldsymbol{Y}_t\}_{t=1,...,T}$ and $\{\boldsymbol{X}_t\}_{t=1,...,T}$ as in (1). Then $\hat{\gamma}^{FGLS}\xrightarrow{P}\gamma$ and*

$$\sqrt{T}\left(\hat{\gamma}^{FGLS}-\gamma\right)\xrightarrow{d}N\left(0,\left[R^{\intercal}\left\{\text{plim}(T^{-1}ZZ^{\intercal})\otimes\hat{\Sigma}_u^{-1}\right\}R\right]^{-1}\right), \tag{7}$$

where $\xrightarrow{P}$ and $\xrightarrow{d}$ denote convergence in probability and distribution, respectively, and plim *is the probability limit.*

4. Definition of the Model Matrix, R

Please refer to the notation in the main paper. From equation (4) we have

$$\underset{N^2\times 1}{\operatorname{vec}(\phi_k)} = \begin{bmatrix}\alpha_{1,k} & \mathbf{0}_N & \alpha_{2,k} & \mathbf{0}_N & \cdots & \alpha_{N,k}\end{bmatrix}^\intercal + \sum_{r=1}^{s_k} \beta_{k,r} \operatorname{vec}\left\{W^{(r)}\right\}, \tag{8}$$

$$\operatorname{vec}(\Lambda_k) = \lambda_k \operatorname{vec}(I_N), \tag{9}$$

where $[\mathbf{x}]_i$ denotes the ith element of $\mathbf{x}$ and $\mathbf{0}_a$ denotes the length a-vector of zeros.

By vertically stacking the $\operatorname{vec}(\phi_k)$ and $\operatorname{vec}(\Lambda_k)$ vectors, the $P \times M$ matrix R is

$$\underset{N^2(p+p'+1)\times M}{R} = \begin{bmatrix}
A & R_1 & 0_{N^2\times N} & 0_{N^2\times s_2} & \cdots \\
0_{N^2\times N} & 0_{N^2\times s_1} & A & R_2 & \cdots \\
\vdots & \vdots & \vdots & \vdots & \\
0_{N^2\times N} & 0_{N^2\times N} & 0_{N^2\times s_1} & 0_{N^2\times s_2} & \cdots \\
0_{N^2\times N} & 0_{N^2\times N} & 0_{N^2\times s_1} & 0_{N^2\times s_2} & \cdots \\
0_{N^2\times N} & 0_{N^2\times N} & 0_{N^2\times s_1} & 0_{N^2\times s_2} & \cdots \\
\vdots & \vdots & \vdots & \vdots & \\
0_{N^2\times N} & 0_{N^2\times N} & 0_{N^2\times s_1} & 0_{N^2\times s_2} & \cdots
\end{bmatrix}
\begin{bmatrix}
\cdots & 0_{N^2\times N} & 0_{N^2\times s_p} & 0 & 0 & \cdots & 0 \\
\cdots & 0_{N^2\times N} & 0_{N^2\times s_p} & 0 & 0 & \cdots & 0 \\
 & \vdots & \vdots & \vdots & \vdots & & \vdots \\
\cdots & A & R_p & 0 & 0 & \cdots & 0 \\
\cdots & 0_{N^2\times N} & 0_{N^2\times s_p} & L & \mathbf{0}_{N^2} & \cdots & \mathbf{0}_{N^2} \\
\cdots & 0_{N^2\times N} & 0_{N^2\times s_p} & \mathbf{0}_{N^2} & L & \cdots & \mathbf{0}_{N^2} \\
 & \vdots & \vdots & \vdots & \vdots & \ddots & \vdots \\
\cdots & 0_{N^2\times N} & 0_{N^2\times s_p} & \mathbf{0}_{N^2} & \mathbf{0}_{N^2} & \cdots & L
\end{bmatrix}, \tag{10}$$

where $0_{a\times b}$ denotes the $a \times b$ matrix of zeroes, $\underset{N^2\times s_k}{R_k} = \left[\operatorname{vec}\left\{W^{(1)}\right\}, \ldots, \operatorname{vec}\left\{W^{(s_k)}\right\}\right]$, $\underset{N^2\times 1}{L} = \left[1, \mathbf{0}_N^\intercal, 1, \mathbf{0}_N^\intercal, 1, \ldots, 1\right]^\intercal$ and $\underset{N^2\times N}{A} = [\mathbf{e}_1, 0_{N\times N}, \mathbf{e}_2, 0_{N\times N}, \mathbf{e}_3, \ldots, \mathbf{e}_N]^\intercal$.

Part 2: Exploratory Data Analysis

5. Second-order stationary tests

We used the second-order stationary test from Nason (2013, 2016) on the demeaned purchasing managers' indices from each country. The results are summarised by Figures 1 to 13. Outside of COVID and, in a few cases, the great financial crisis, there is little evidence to reject the null hypothesis of second-order stationarity. Table 1 shows which countries had no non-stationarities, those that exhibited non-stationarities during the COVID-19 pandemic and those that exhibited them during the COVID-19 pandemic and great financial crisis.

Although some of these time series do exhibit non-stationarities, for forecasting the 2007–08 global financial crisis was about 160 time periods ago, was relatively short-lived (with respect

Table 1. Countries' PMI non-stationarity status.

Non-stationarity type	Countries
None	USA, Japan, India, China, Brazil, Australia
COVID only	Spain, Italy, Germany, France
COVID + GFC	UK, Russia, Ireland

to the extent of the rest of the data) and will not unduly influence the forecasts (the methods we are using place greater weight on more recent observations). Secondly, the non-stationarities due to the COVID-19 are precisely what we expect the exogenous variables to model — they, in effect, act as a kind of intervention variables.

6. Covariate plots

Below, Figures 14 to 25 show the plots of covariates for all country nodes, excluding the UK (which can be found in the main article as Figure 2). All series have been standardised to zero mean and unit variance so that they may be plotted on the same axes.

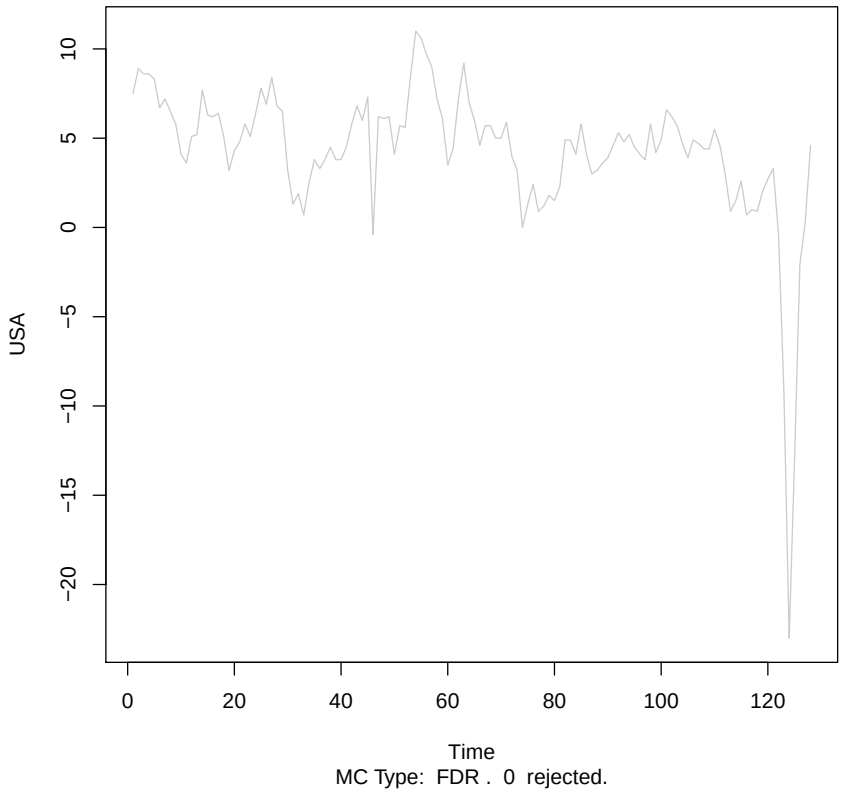

Fig. 1. Stationarity test plot for USA PMIs. No formal non-stationarities discovered

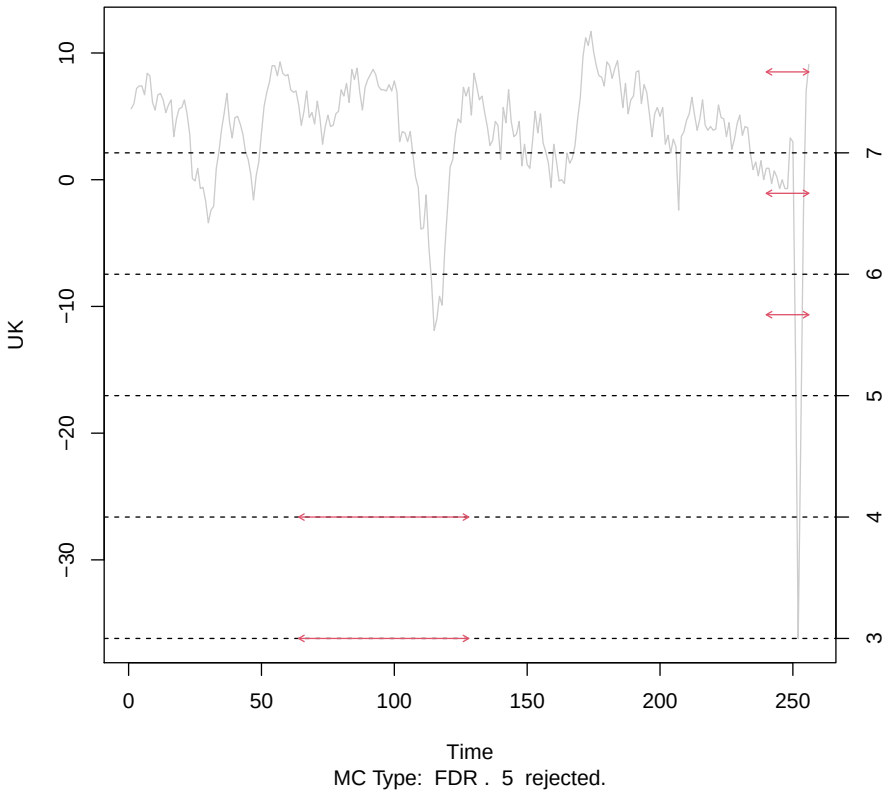

Fig. 2. Stationarity test plot for UK PMIs. Non-stationarities discovered during the great financial crisis and COVID-19.

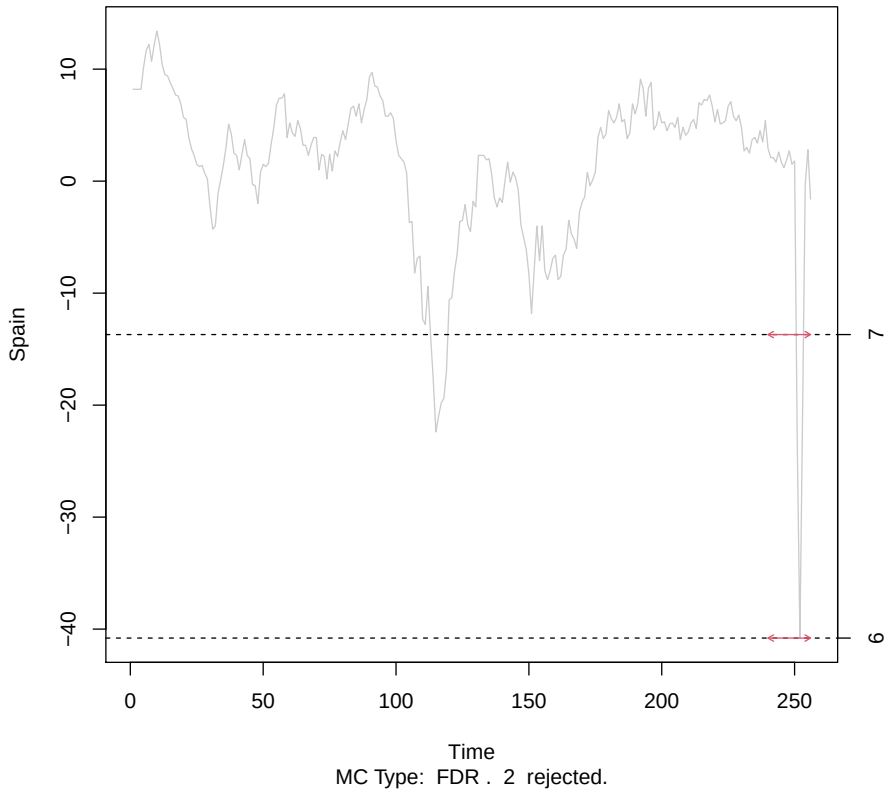

Fig. 3. Stationarity test plot for Spanish PMIs. Non-stationarities discovered during COVID-19.

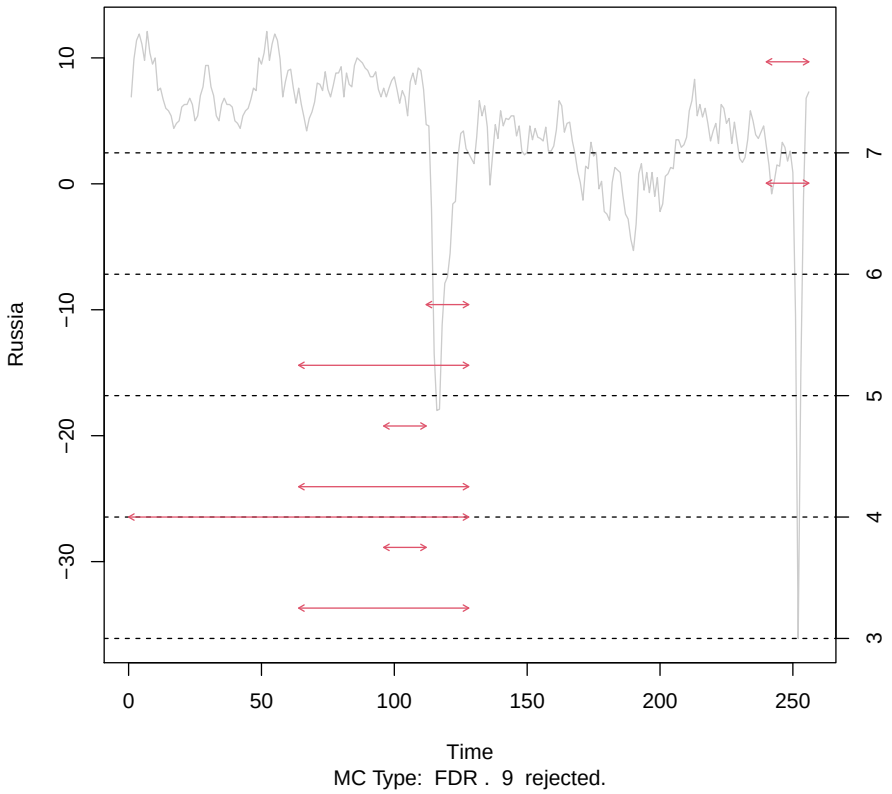

Fig. 4. Stationarity test plot for Russian PMIs. Non-stationarities discovered during the great financial crisis and COVID-19.

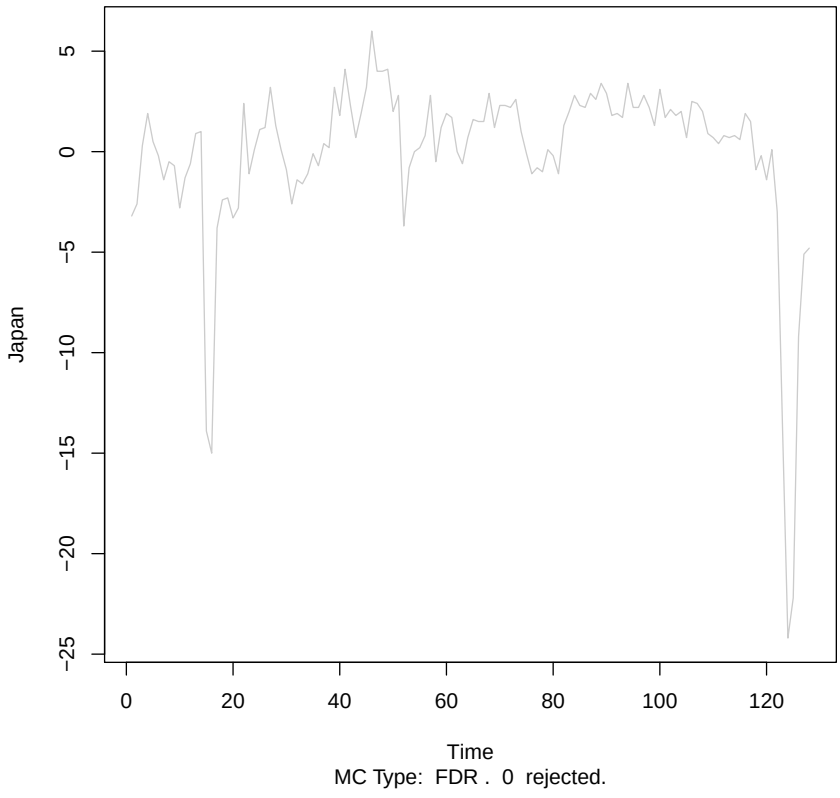

[p]

Fig. 5. Stationarity test plot for Japanese PMIs. No formal non-stationarities discovered

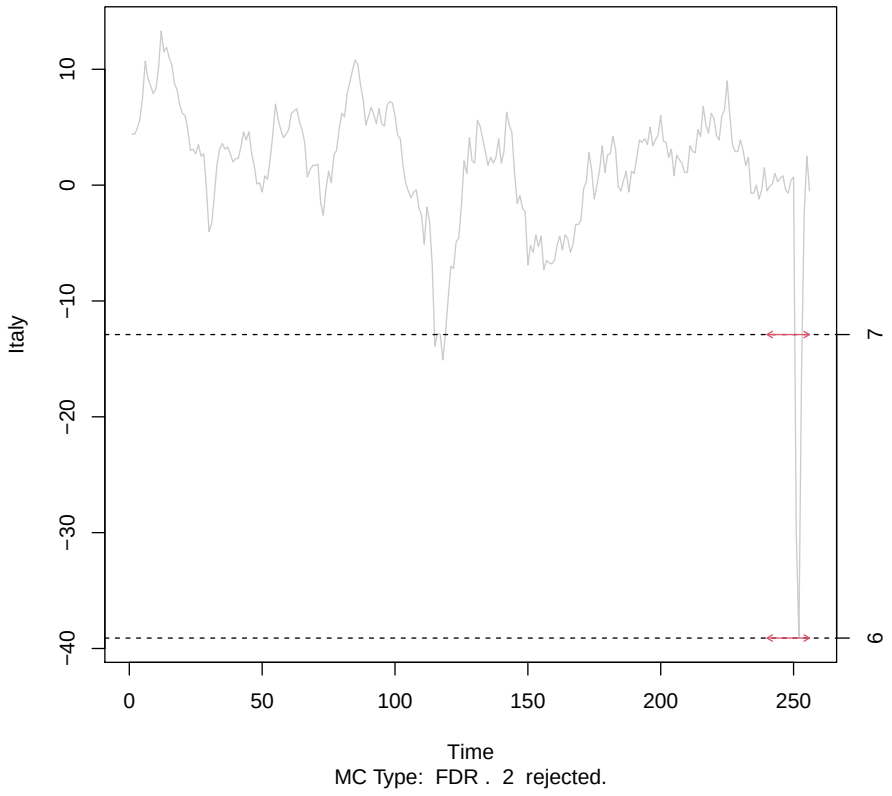

[p]

Fig. 6. Stationarity test plot for Italian PMIs. Non-stationarities discovered during COVID-19.

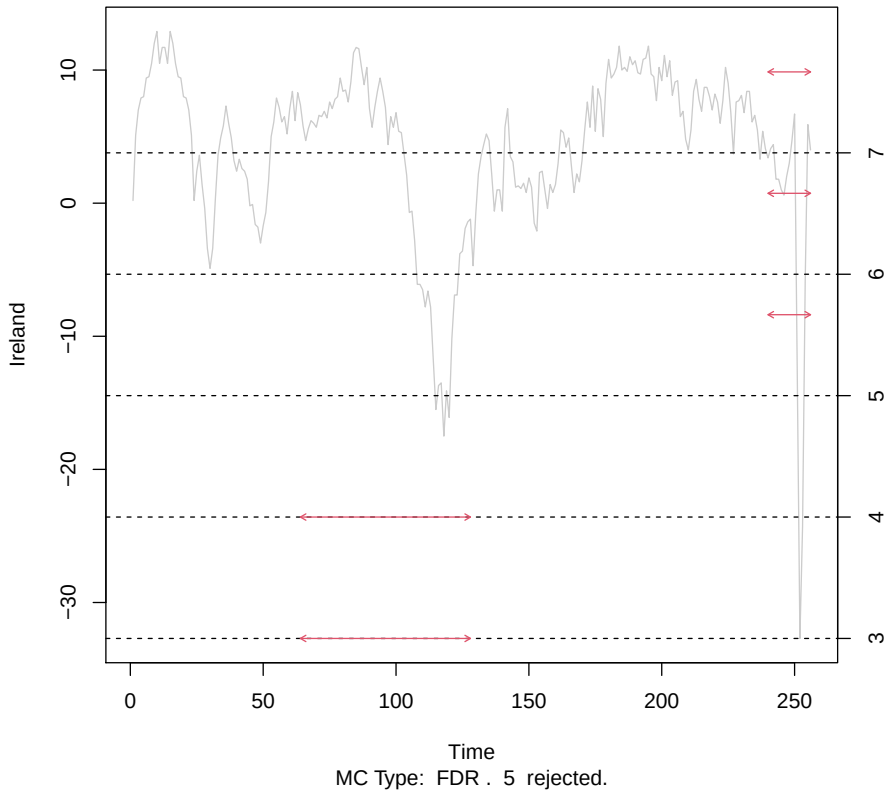

Fig. 7. Stationarity test plot for Irish PMIs. Non-stationarities discovered during the great financial crisis and COVID-19.

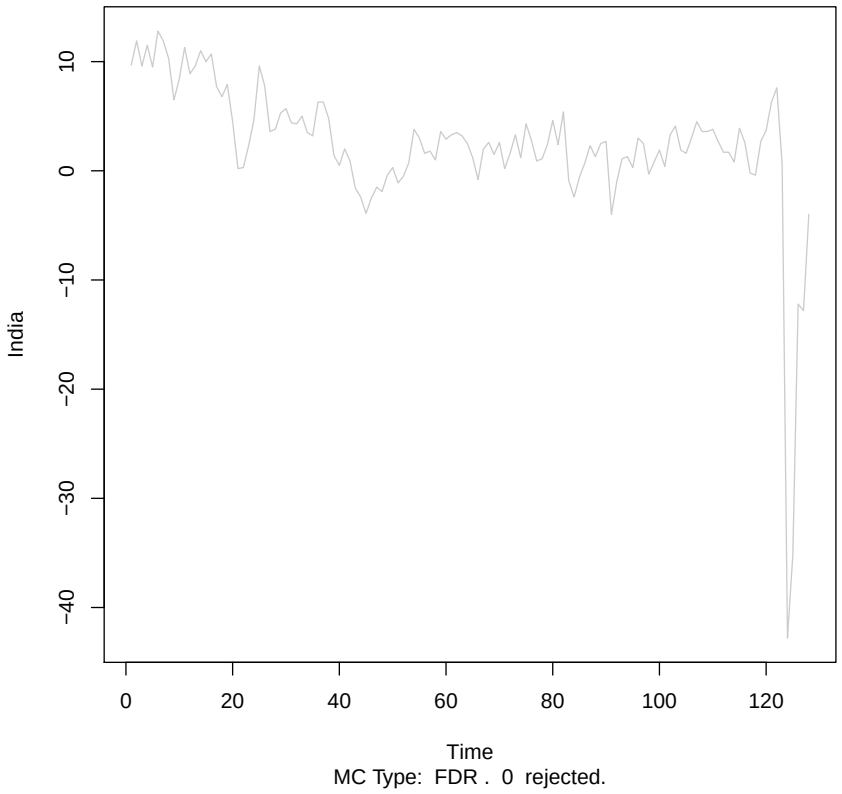

Fig. 8. Stationarity test plot for Indian PMIs. No formal non-stationarities discovered

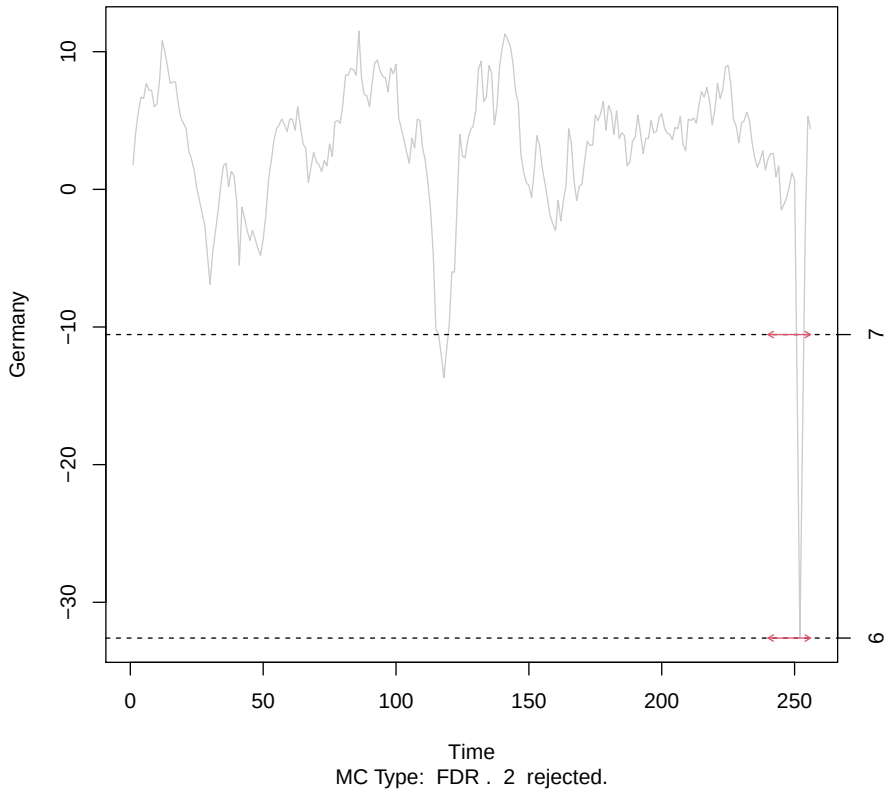

Fig. 9. Stationarity test plot for German PMIs. Non-stationarities discovered during COVID-19.

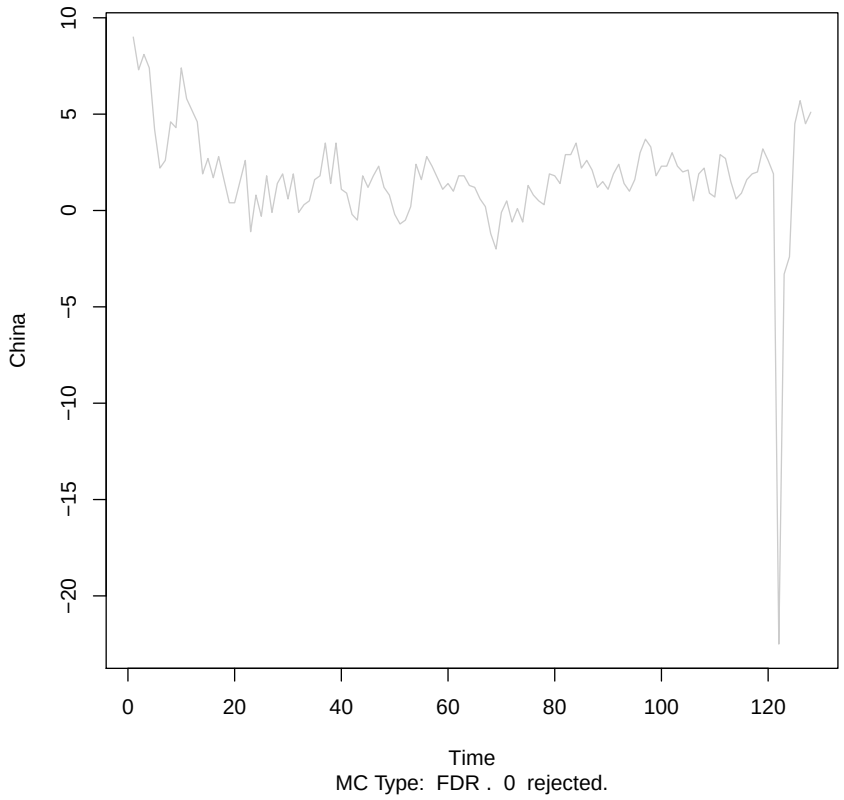

Fig. 10. Stationarity test plot for Chinese PMIs. No formal non-stationarities discovered

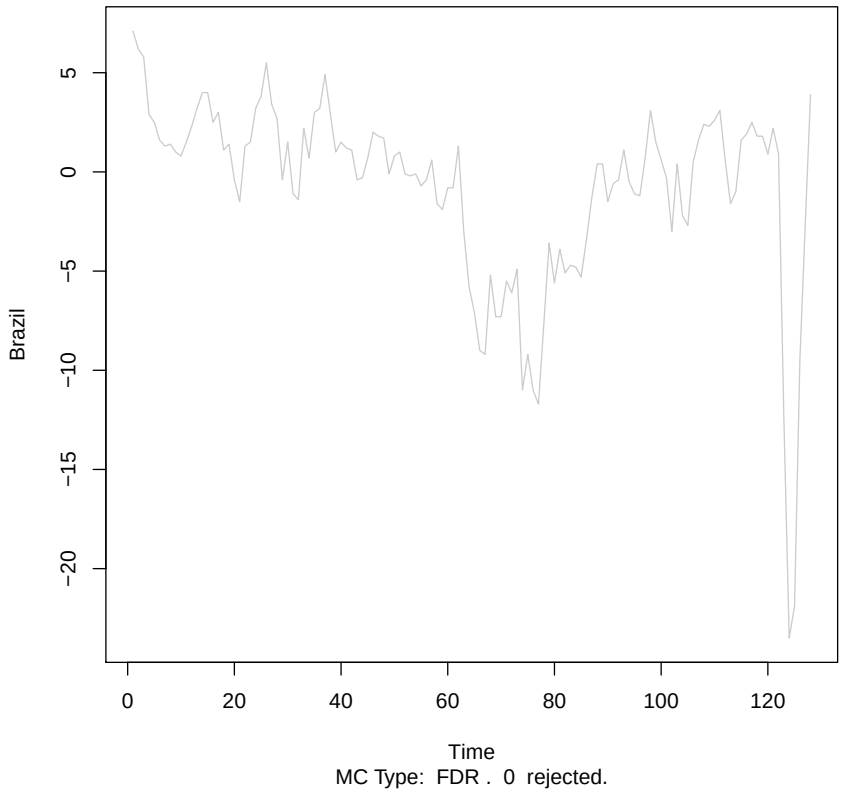

Fig. 11. Stationarity test plot for Brazilian PMIs. No formal non-stationarities discovered

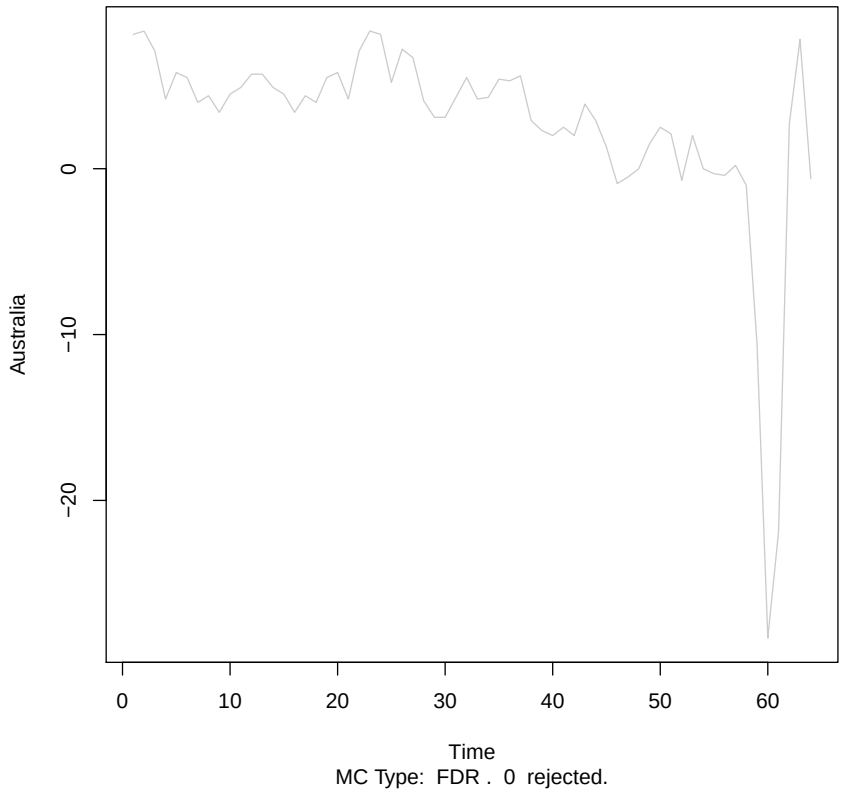

Fig. 12. Stationarity test plot for Australian PMIs. No formal non-stationarities discovered

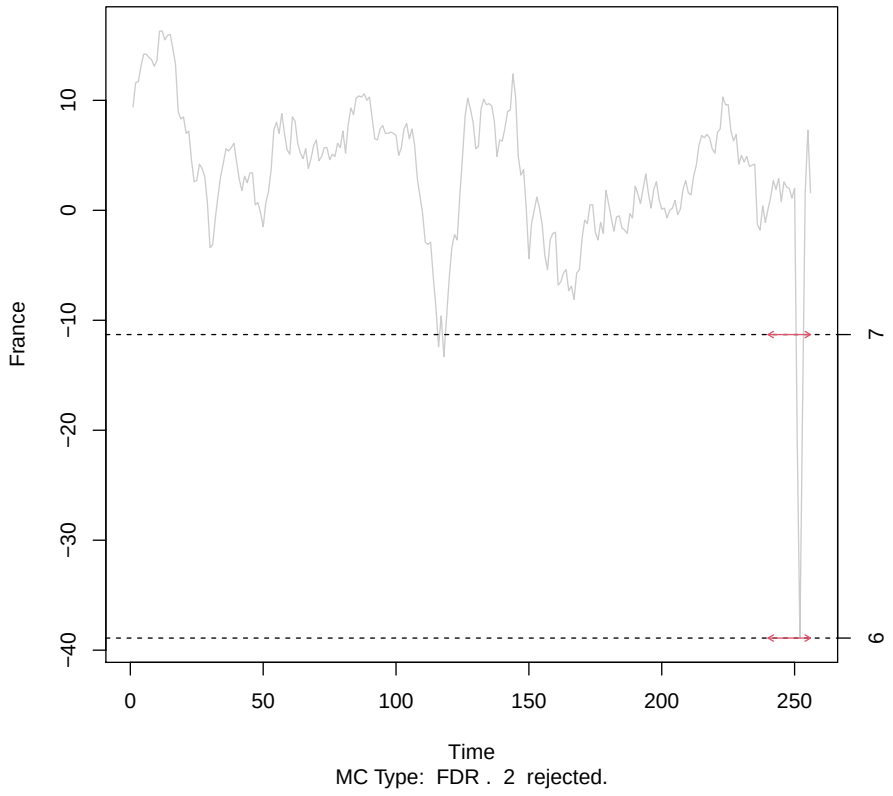

Fig. 13. Stationarity test plot for French PMIs. Non-stationarities discovered during COVID-19.

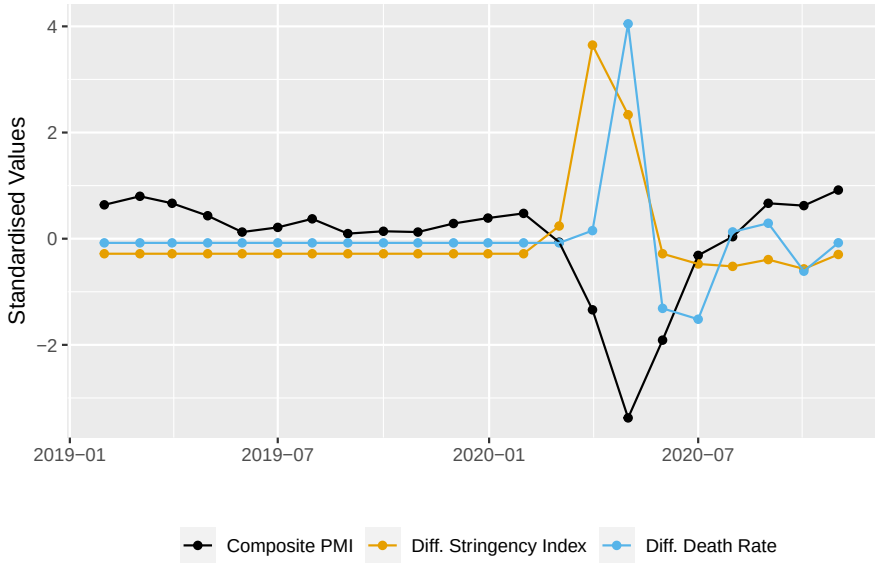

Fig. 14. Plot of US Composite PMI together with US stringency index and US death rate covariates, where all variables have been standardised to zero mean and unit variance.

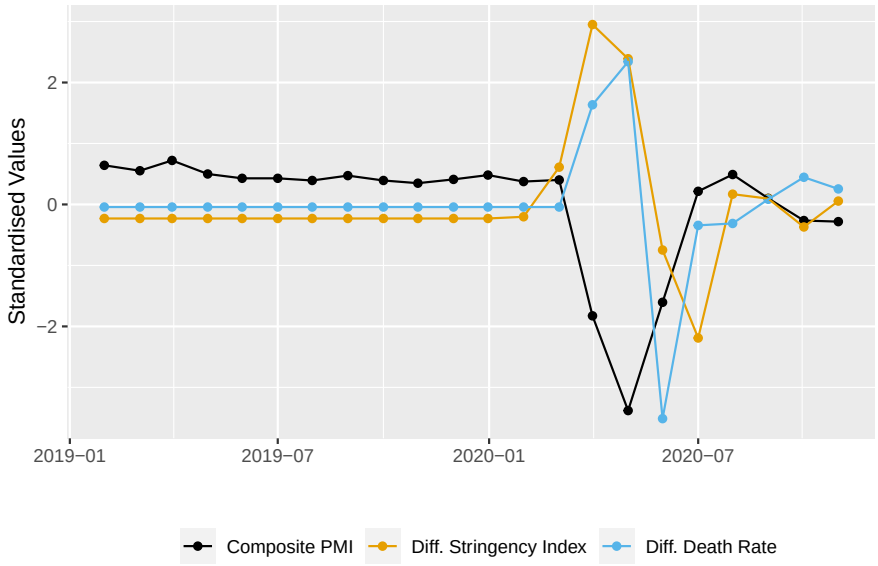

Fig. 15. Plot of Spain Composite PMI together with Spain stringency index and Spain death rate covariates, where all variables have been standardised to zero mean and unit variance.

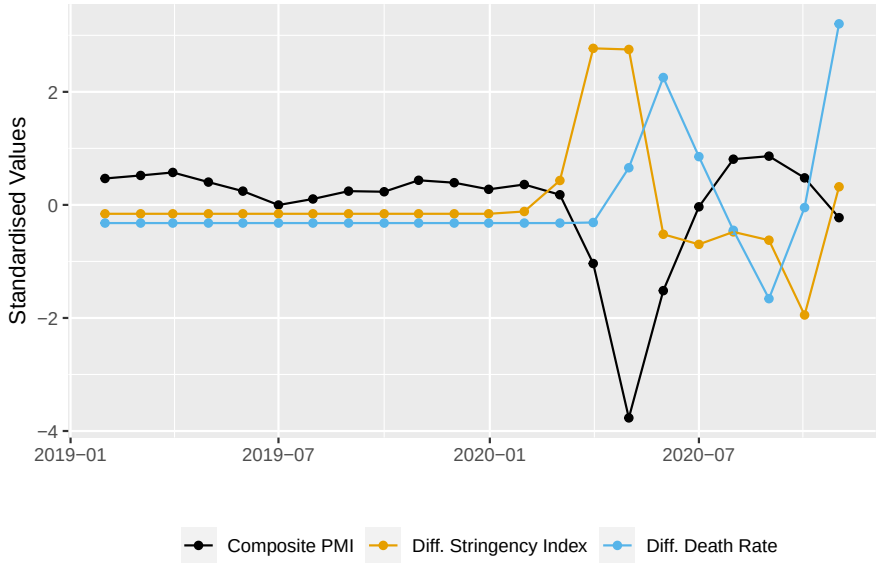

Fig. 16. Plot of Russia Composite PMI together with Russia stringency index and Russia death rate covariates, where all variables have been standardised to zero mean and unit variance.

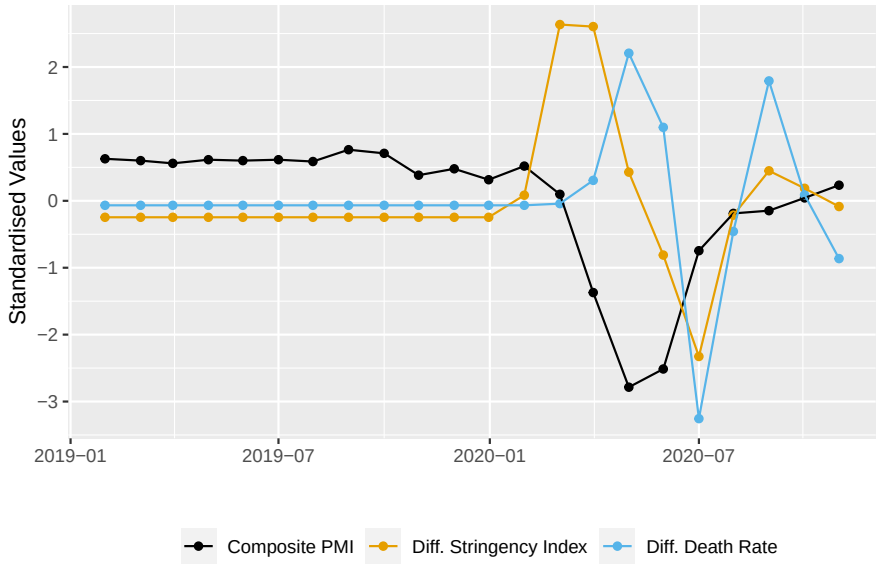

Fig. 17. Plot of Japan Composite PMI together with Japan stringency index and Japan death rate covariates, where all variables have been standardised to zero mean and unit variance.

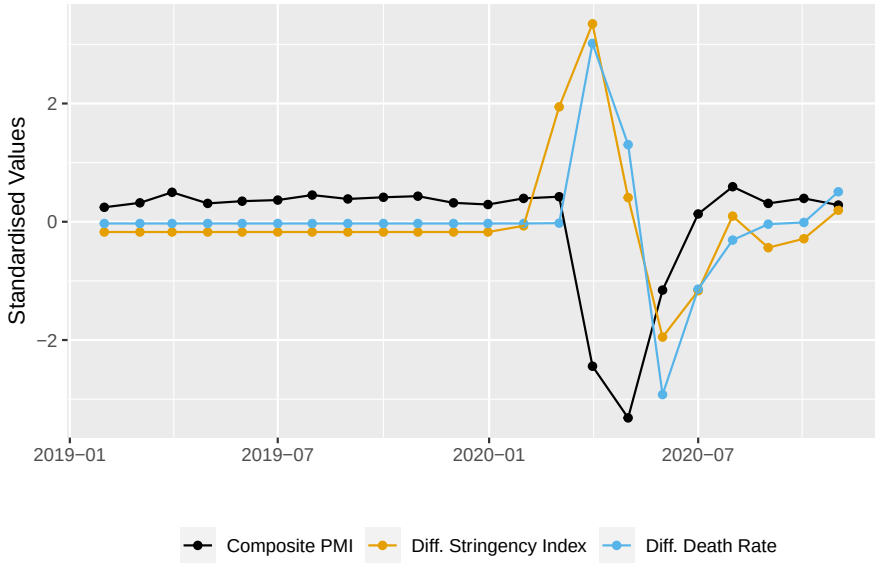

Fig. 18. Plot of Italy Composite PMI together with Italy stringency index and Italy death rate covariates, where all variables have been standardised to zero mean and unit variance.

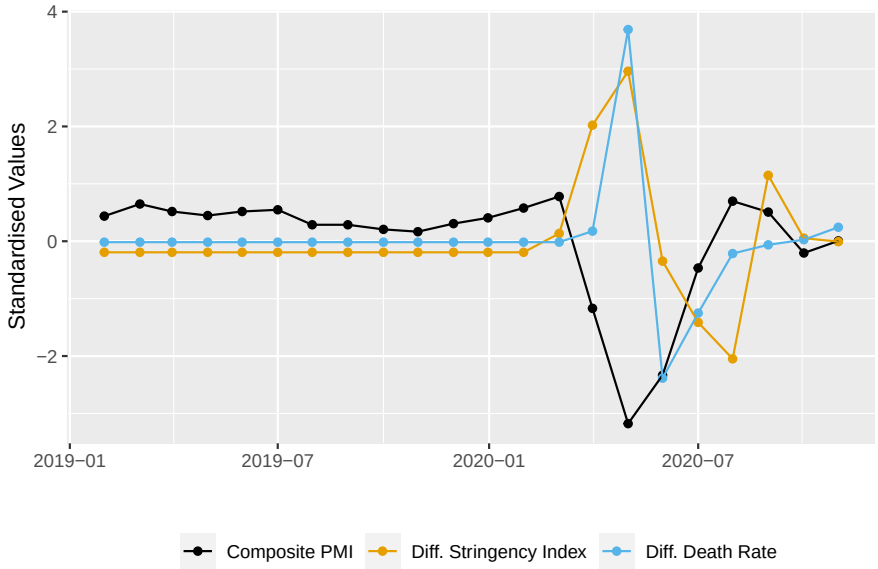

Fig. 19. Plot of Ireland Composite PMI together with Ireland stringency index and Ireland death rate covariates, where all variables have been standardised to zero mean and unit variance.

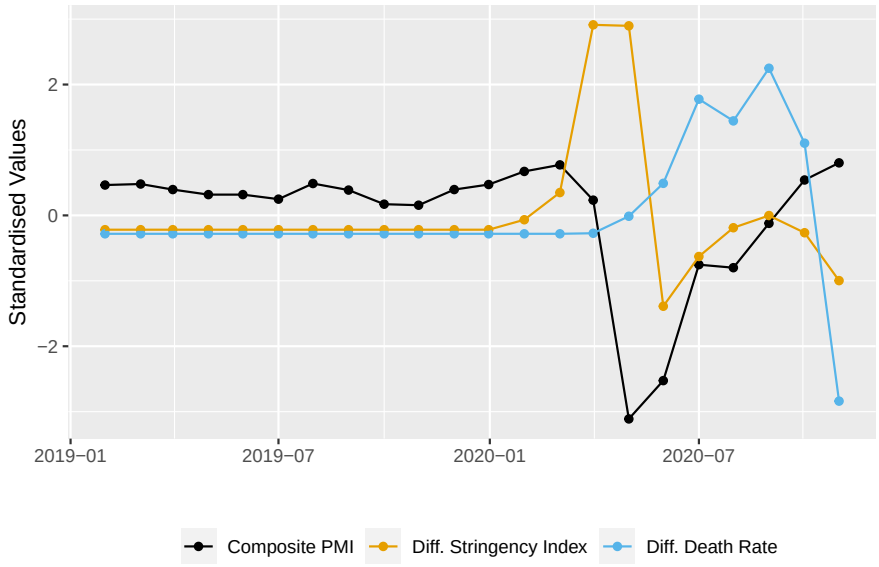

Fig. 20. Plot of India Composite PMI together with India stringency index and India death rate covariates, where all variables have been standardised to zero mean and unit variance.

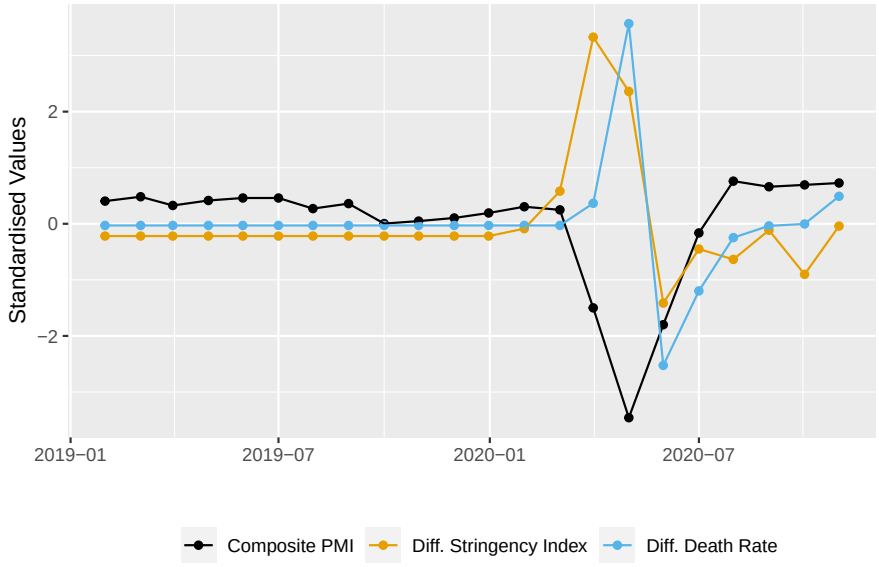

Fig. 21. Plot of Germany Composite PMI together with Germany stringency index and Germany death rate covariates, where all variables have been standardised to zero mean and unit variance.

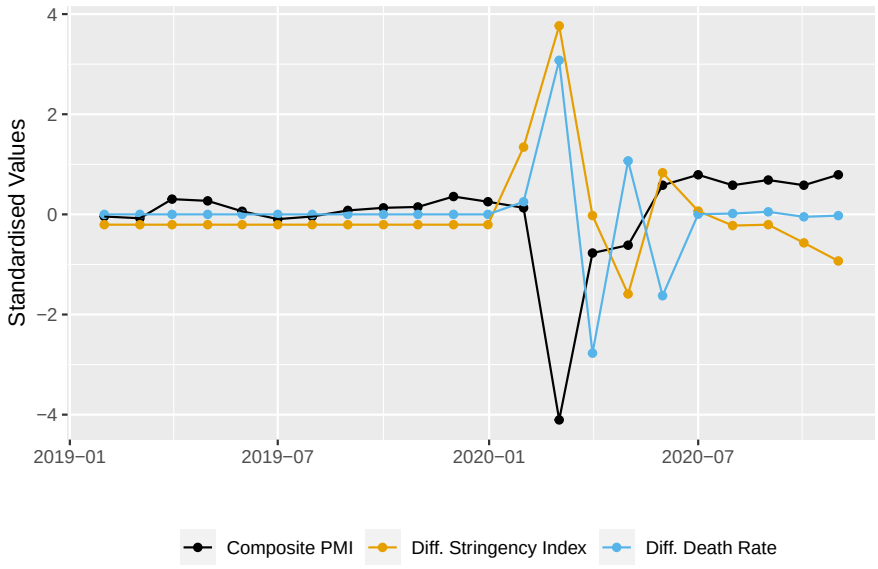

Fig. 22. Plot of China Composite PMI together with China stringency index and China death rate covariates, where all variables have been standardised to zero mean and unit variance.

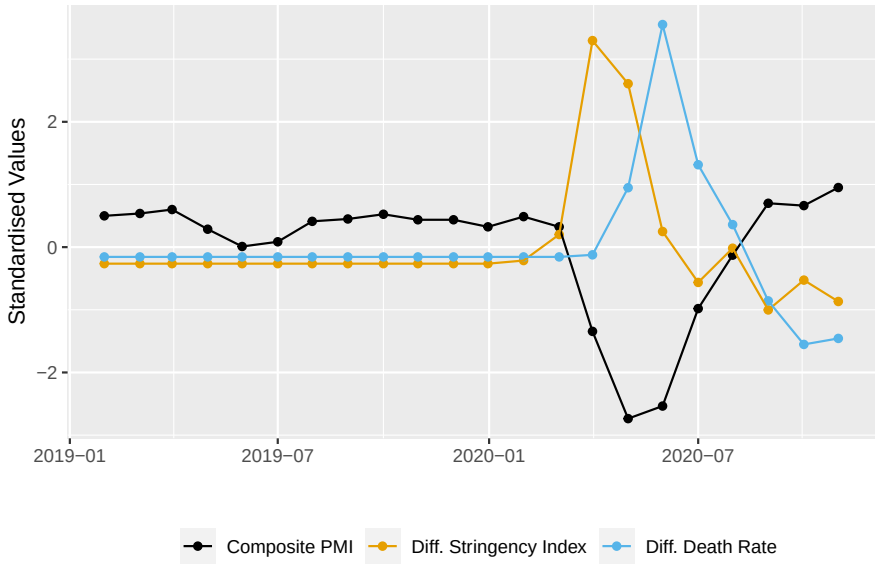

Fig. 23. Plot of Brazil Composite PMI together with Brazil stringency index and Brazil death rate covariates, where all variables have been standardised to zero mean and unit variance.

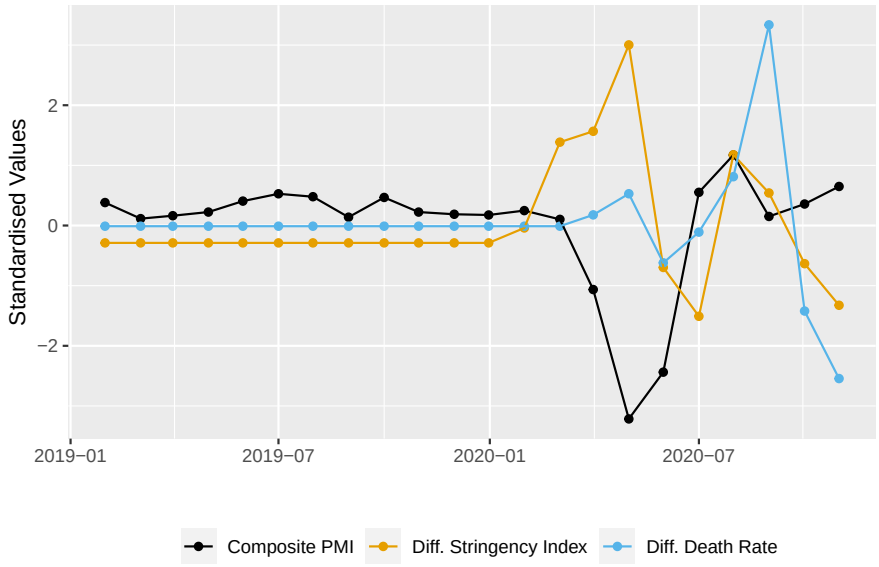

Fig. 24. Plot of Australia Composite PMI together with Australia stringency index and Australia death rate covariates, where all variables have been standardised to zero mean and unit variance.

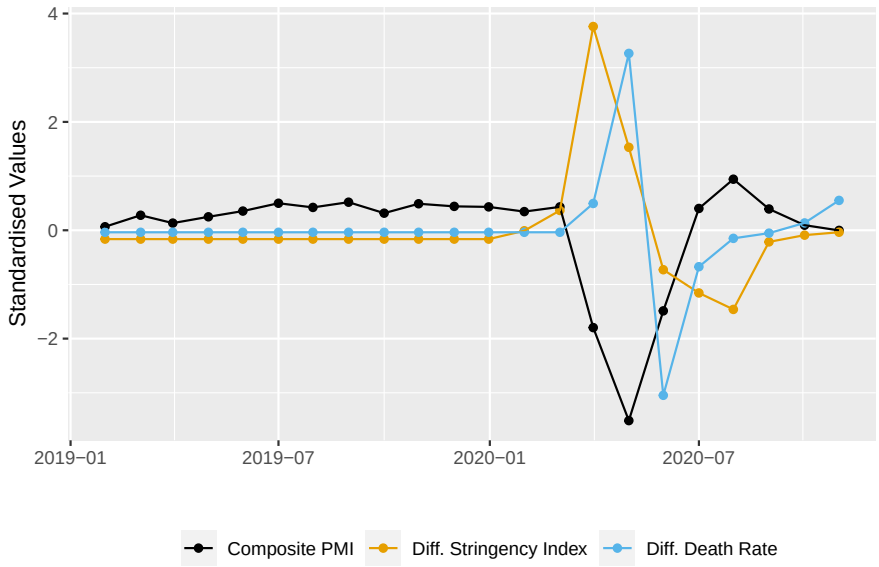

Fig. 25. Plot of France Composite PMI together with France stringency index and France death rate covariates, where all variables have been standardised to zero mean and unit variance.

Table 2. Out-of-sample composite PMI forecast performance between Jan-18 and Oct-20 using GNAR, VAR and naive forecasting. MSFE=Out-of-sample mean-squared forecasting error; SE = standard error

Model	Model order	Parameters	MSFE (SE)
Global-α GNAR, fully-connected net	1, (1)	2	38.2 (6.8)
Global-α GNAR, nearest-neighbour net	1, (0)	1	38.8 (7.0)
Local-α GNAR, fully-connected net	1, (1)	13	38.5 (6.8)
Local-α GNAR, nearest-neighbour net	1, (0)	12	39.1 (7.0)
VAR	1	144	40.7 (8.0)
AR	1	12	39.1 (7.0)
Naive forecast	-	-	40.6 (7.2)

Part 3: GNAR and GNARX experiments

7. Additional GNAR experimental results

Figures 26-37 plot the out-of-sample one-step-ahead rolling forecasts of the local-α GNAR$(1, (1))$ model between Jan-18 and Oct-20 using the fully connected trade network (i.e. the GNAR specification with lowest mean-squared forecast error), together with the forecasts of the VAR(2) model. The forecasts are arranged in order of 2019 country GDP.

Table 2 shows the performance of the models selected by optimising for MSFE, rather than BIC. Specifically, models of all orders up to $p = 3$ were fit on the first 180 months of the in-sample period and their corresponding forecast errors were recorded for the remaining 60 months of the in-sample period. Model orders were selected to minimise the MSFE computed from these forecast errors. The resulting GNAR models using the fully-connected networks outperform both the VAR model and the univariate AR models in terms of MSFE.

8. Simulation results for GNARX model order selection using BIC optimisation

We simulate network time series data of three different lengths T from a local-α GNARX(1, (1), 1) model with the fiveNet network used in the simulation experiments of Leeming (2019). Parameters are set as $\alpha_{1,1} = 0.4, \alpha_{2,1} = \alpha_{4,1} = \alpha_{5,1} = 0.2, \alpha_{3,1} = 0.4, \beta_{1,1} = 0.5, \lambda_{1,1} = 0.4, \lambda_{1,2} = 0.2$. Both the GNARX innovations and the exogenous regressor are sampled i.i.d from a standard normal distribution. These settings guarantee stationarity of the resulting process.

Tables 3 and 4 show that, as the lengths of the time series increases, the correct model order is identified with increasing probability using both global BIC optimisation and our stagewise approach. The latter approach, which we adopt in our PMI forecasting experiments, involves first selecting autoregressive order p while ignoring the network. Once p has been selected, we optimise on the remaining components of the model order. To ensure computational feasibility, for global BIC optimisation we have set order limits of $p = p' = 3$. For stagewise optimisation, we are able to set a higher limit of $p = 12$.

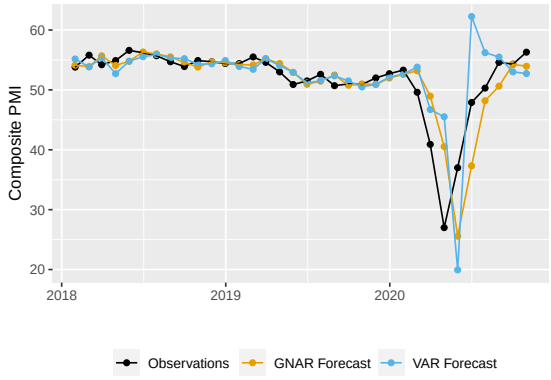

Fig. 26. United States: Out-of-sample one-step-ahead rolling composite PMI forecasts of the local-α GNAR$(1, 1)$ model and the VAR(2) model.

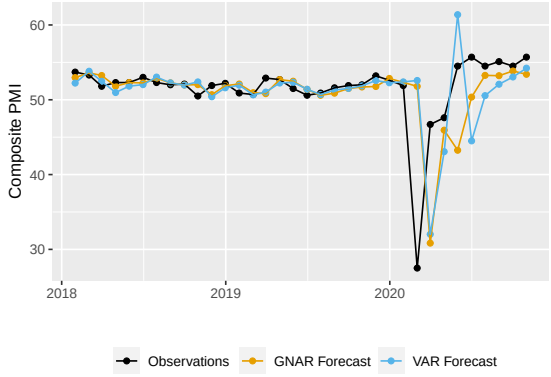

Fig. 27. China: Out-of-sample one-step-ahead rolling composite PMI forecasts of the local-α GNAR$(1, 1)$ model and the VAR(2) model.

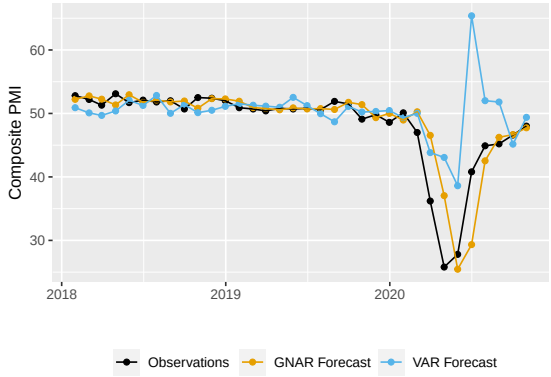

Fig. 28. Japan: Out-of-sample one-step-ahead rolling composite PMI forecasts of the local-α GNAR$(1, 1)$ model and the VAR(2) model.

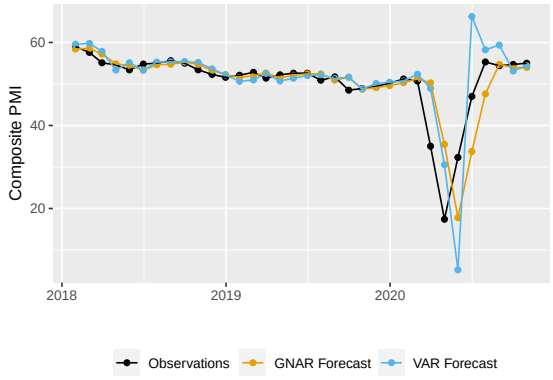

Fig. 29. Germany: Out-of-sample one-step-ahead rolling composite PMI forecasts of the local-α GNAR$(1,1)$ model and the VAR(2) model.

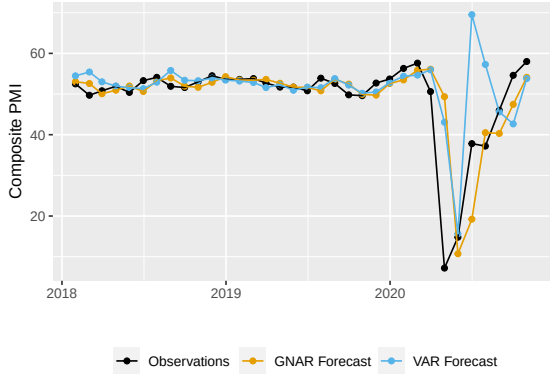

Fig. 30. India: Out-of-sample one-step-ahead rolling composite PMI forecasts of the local-α GNAR$(1,1)$ model and the VAR(2) model.

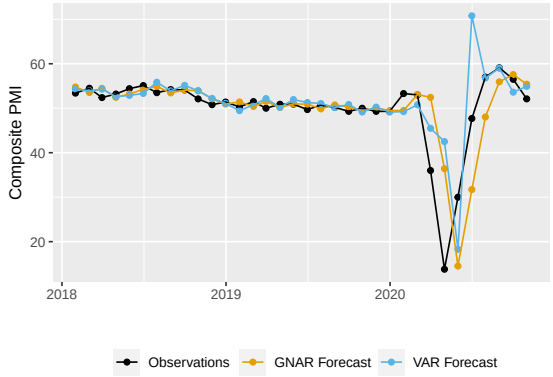

Fig. 31. United Kingdom: Out-of-sample one-step-ahead rolling composite PMI forecasts of the local-α GNAR$(1,1)$ model and the VAR(2) model.

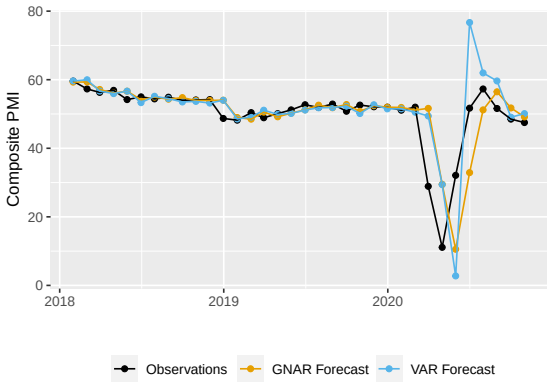

Fig. 32. France: Out-of-sample one-step-ahead rolling composite PMI forecasts of the local-α GNAR$(1, 1)$ model and the VAR(2) model.

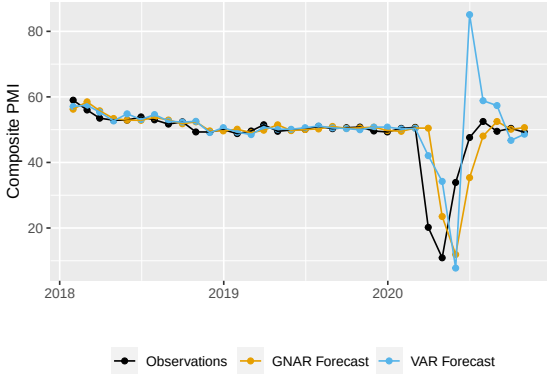

Fig. 33. Italy: Out-of-sample one-step-ahead rolling composite PMI forecasts of the local-α GNAR$(1, 1)$ model and the VAR(2) model.

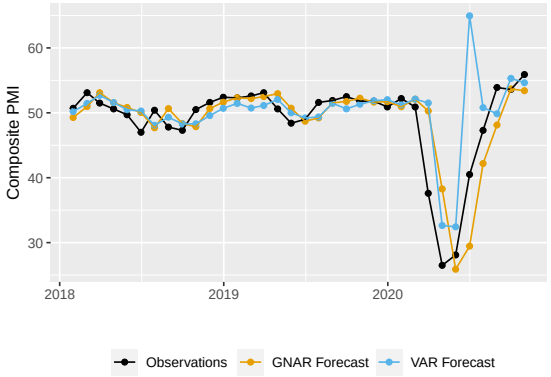

Fig. 34. Brazil: Out-of-sample one-step-ahead rolling composite PMI forecasts of the local-α GNAR$(1, 1)$ model and the VAR(2) model.

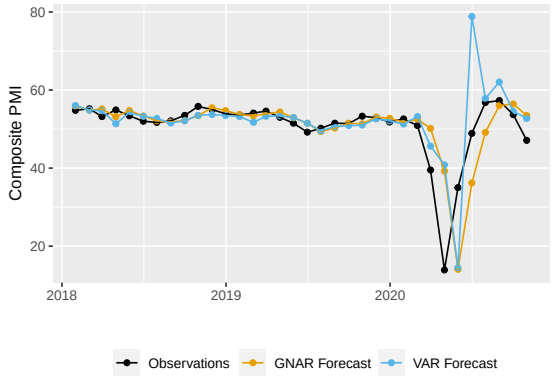

Fig. 35. Russia: Out-of-sample one-step-ahead rolling composite PMI forecasts of the local-α GNAR$(1,1)$ model and the VAR(2) model.

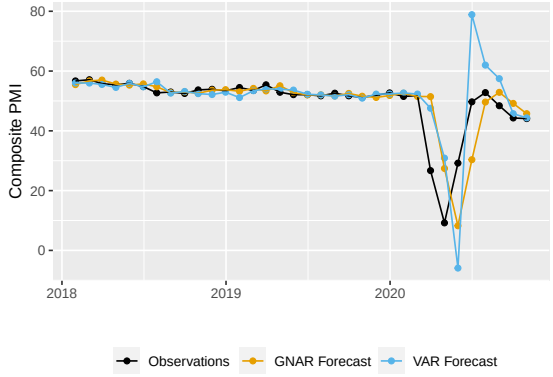

Fig. 36. Spain: Out-of-sample one-step-ahead rolling composite PMI forecasts of the local-α GNAR$(1,1)$ model and the VAR(2) model.

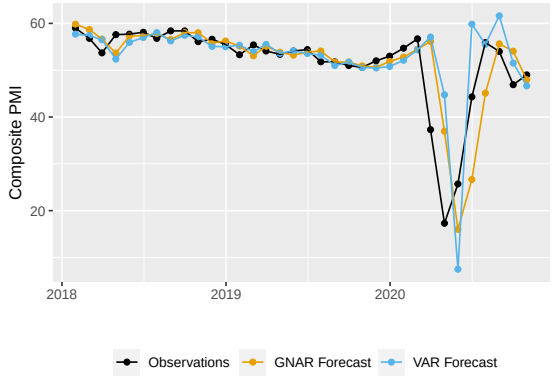

Fig. 37. Ireland: Out-of-sample one-step-ahead rolling composite PMI forecasts of the local-α GNAR$(1,1)$ model and the VAR(2) model.

Table 3. Number of times each model order is selected by minimising the BIC out of 1000 simulations up to orders $p = p' = 3$. The true model order has been bolded.

T	(1, [0], 0)	(1, [1], 0)	**(1, [1], 1)**	(1, [1], 2)	(1, [1], 3)	(1, [2], 0)	(1, [2], 1)	(1, [2], 2)	(1, [2], 3)	(1, [3], 1)
32	1	413	**517**	35	6	7	17	1	1	2
64	0	165	**789**	17	2	2	21	1	0	3
128	0	18	**960**	8	0	0	14	0	0	0

Table 4. Number of times each model order is selected by stagewise BIC optimisation out of 1000 simulations up to orders $p = 12, p' = 3$. The true model order has been bolded.

T	(1, [0], 0)	(1, [0], 1)	(1, [1], 0)	**(1, [1], 1)**	(1, [1], 2)	(1, [1], 3)	(1, [2], 0)	(1, [2], 1)	(1, [2], 2)	(1, [2], 3)	(1, [3], 1)
32	3	1	467	**486**	13	3	7	14	0	1	5
64	0	0	170	**796**	12	3	2	15	0	0	2
128	0	0	19	**957**	11	0	0	11	0	0	2

9. GNARX Residual Analysis

In Figures 38-47, we show the GNARX$(5, [1, 0, 1, 0, 1], 3, 2)$ residual analyses for all countries, arranged in order of 2019 country GDP.

10. Additional GNARX experiment charts

Figures 48-60 show the full set of fitted series for the global-α GNARX$(5, [1, 0, 1, 0, 1], 3, 2)$ model using the fully-connected network and stringency indices only over the most recent five-year period, together with the fitted series of the GNAR model of corresponding model order.

11. Full set of GNARX model forecasting results

The complete set of GNARX model forecasting results is shown in Table 5. We have also included the performance of the univariate AR models with and without (current-period) external regressors, whose order was selected based on BIC optimisation without external regressors as mentioned in Section 3.2 of the main report. Again, each node may have different AR coefficients, comparable to the local-α GNARX models.

As a side note, the chosen model orders suggest that the nearest-neighbour network is not an adequate representation of links between countries, losing valuable information by assuming a country's business confidence depends only on its closest trade partner. This finding holds regardless of which external regressors are included and whether or not the global-α assumption is invoked.

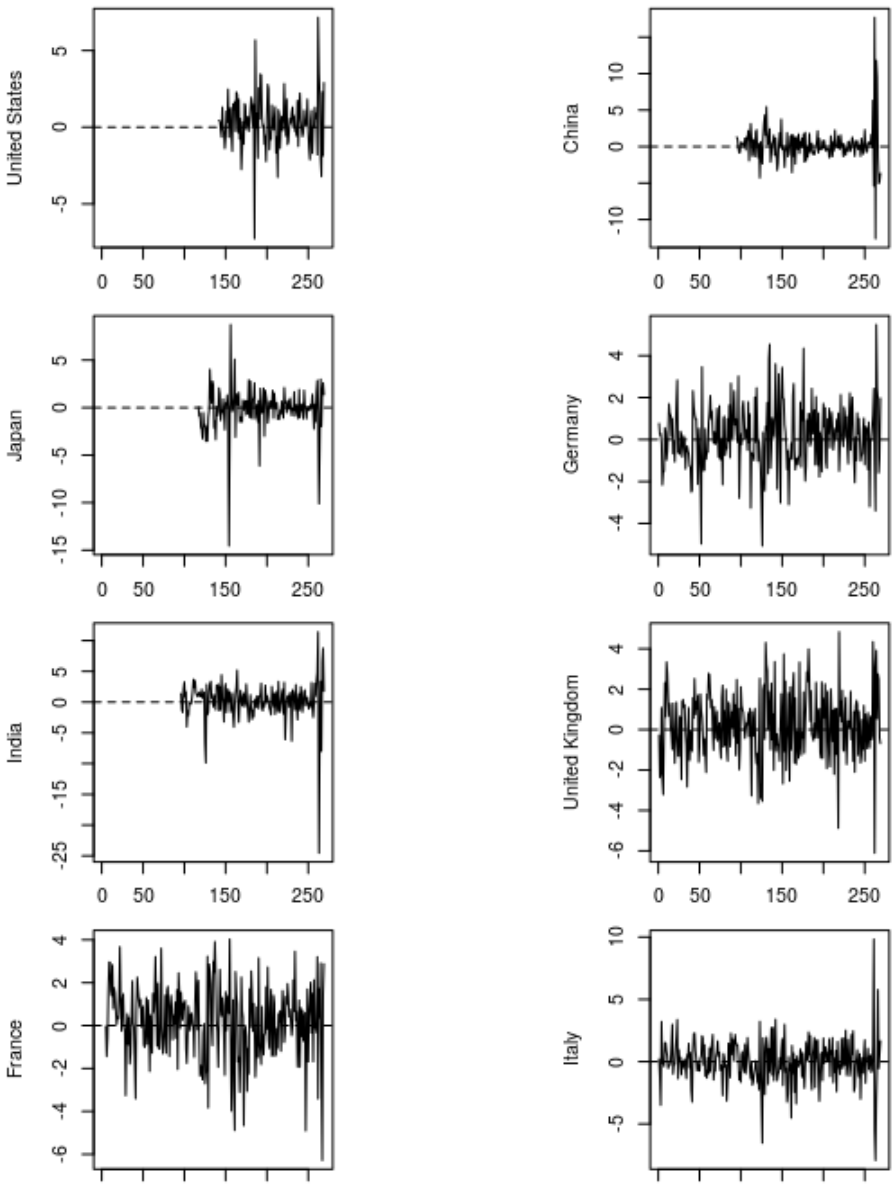

Fig. 38. Time series plots of residuals from best GNARX model. (US, China, Japan, Germany, India, UK, France, Italy)

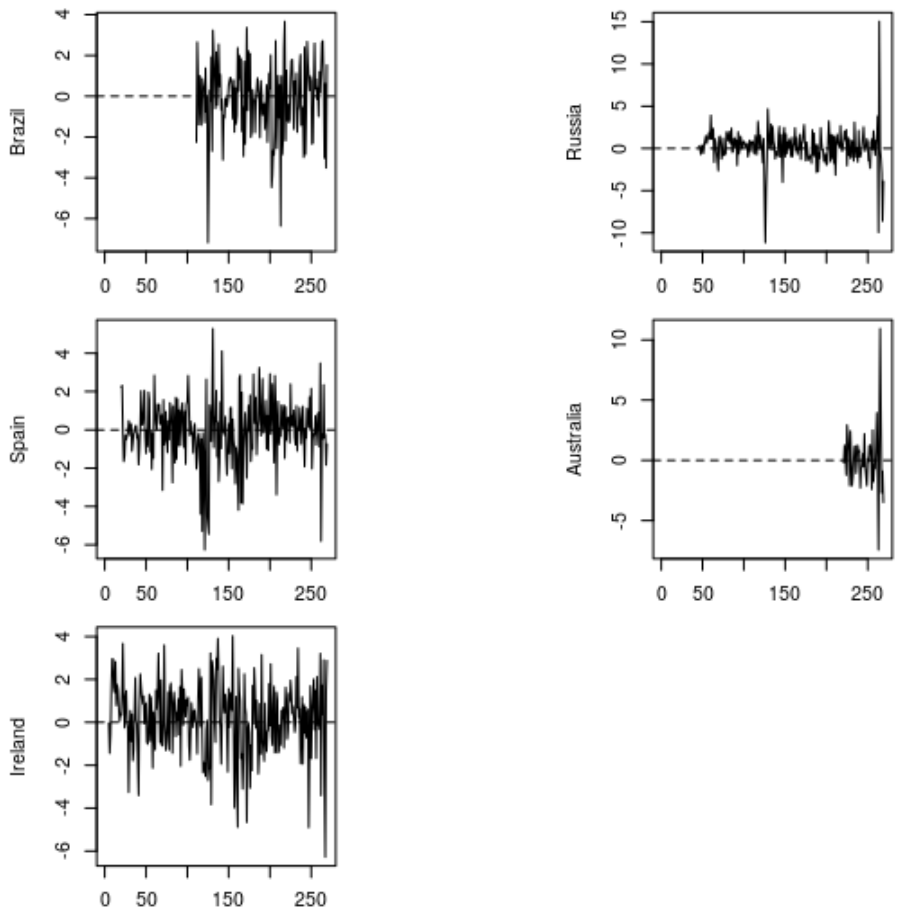

Fig. 39. Time series plots of residuals from best GNARX model. (Brazil, Russia, Spain, Australia, Ireland)

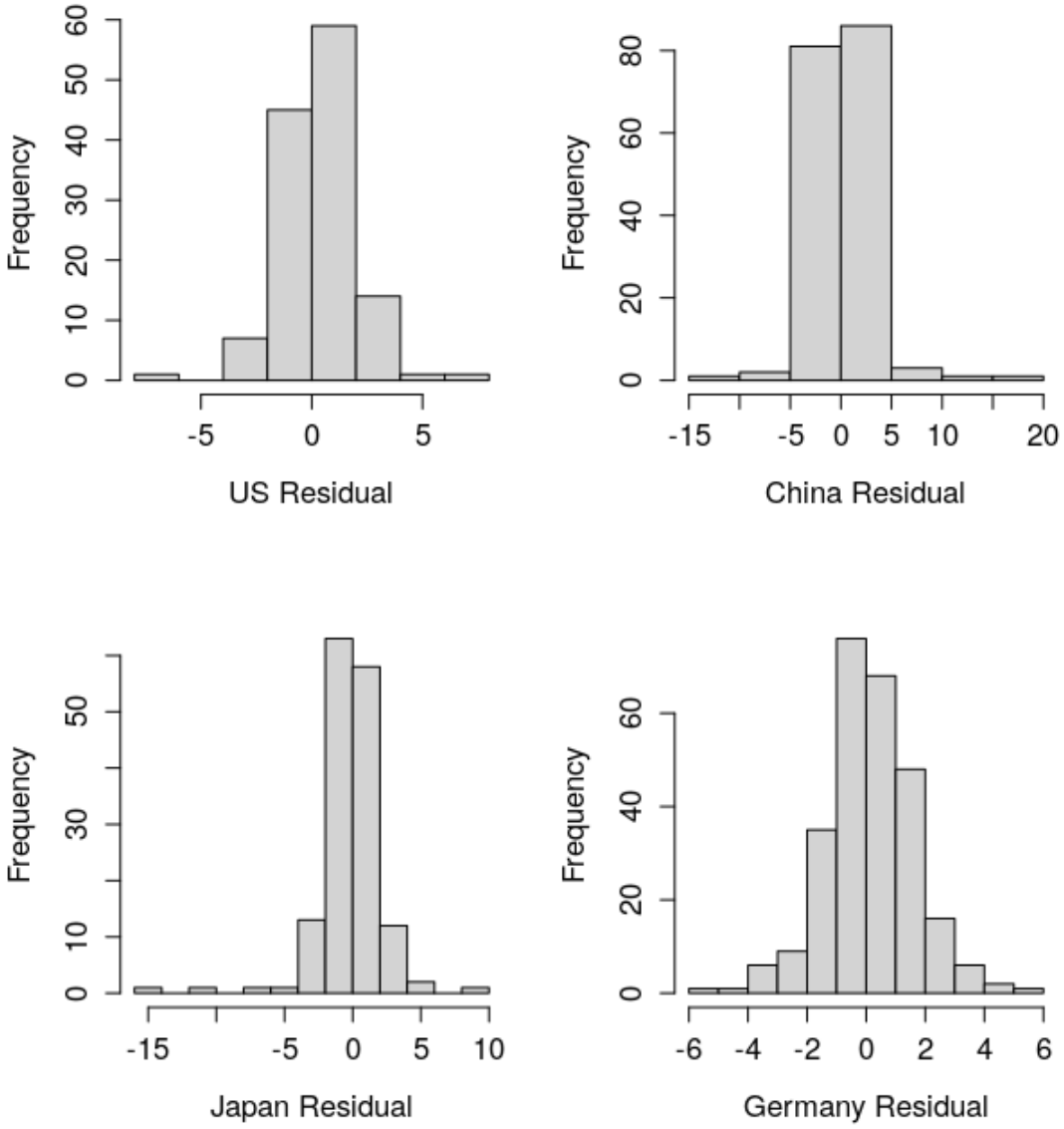

Fig. 40. Histograms of residuals from best GNARX model. (US, China, Japan, Germany)

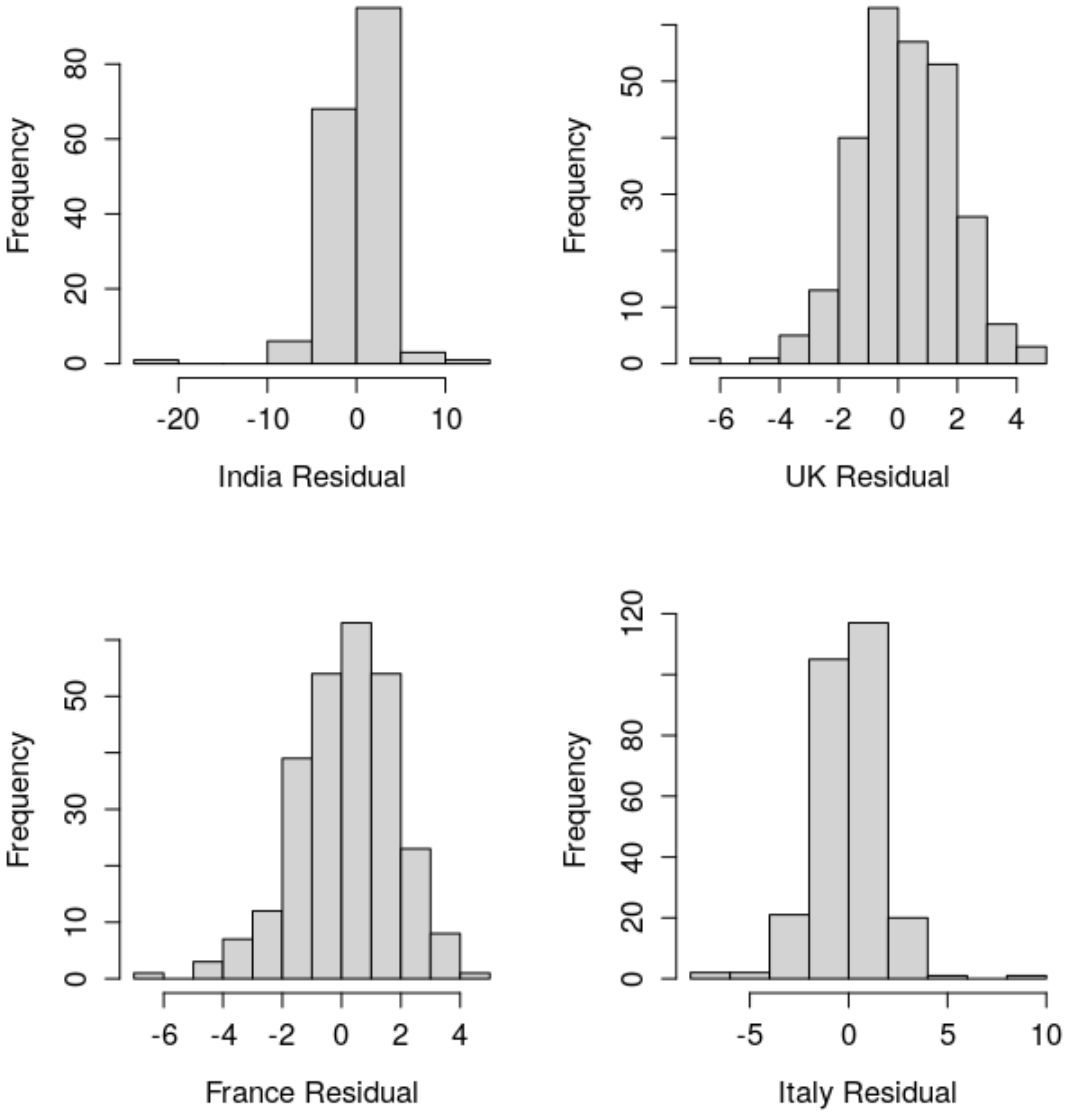

Fig. 41. Histograms of residuals from best GNARX model. (India, UK, France, Italy)

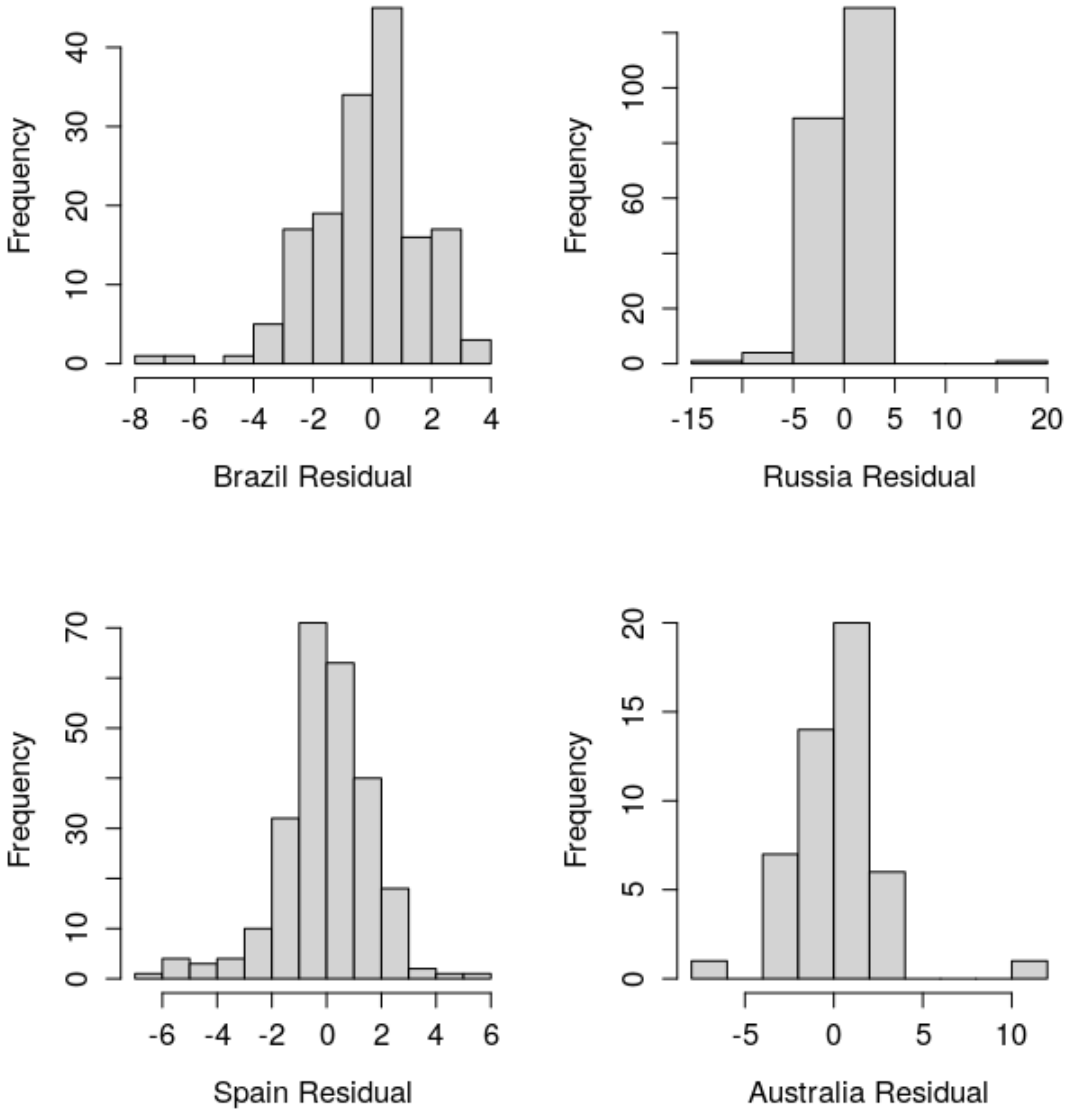

Fig. 42. Histograms of residuals from best GNARX model. (Brazil, Russia, Spain, Australia)

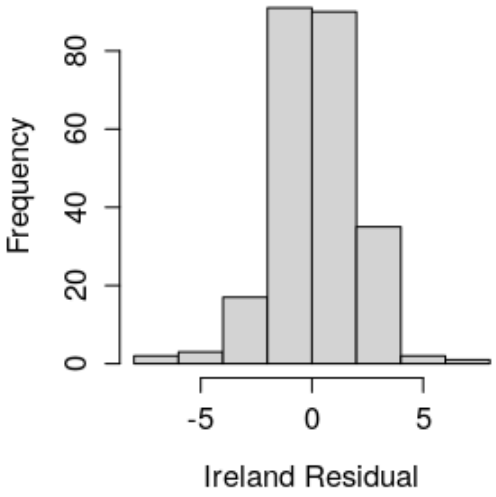

Fig. 43. Histograms of residuals from best GNARX model. (Ireland)

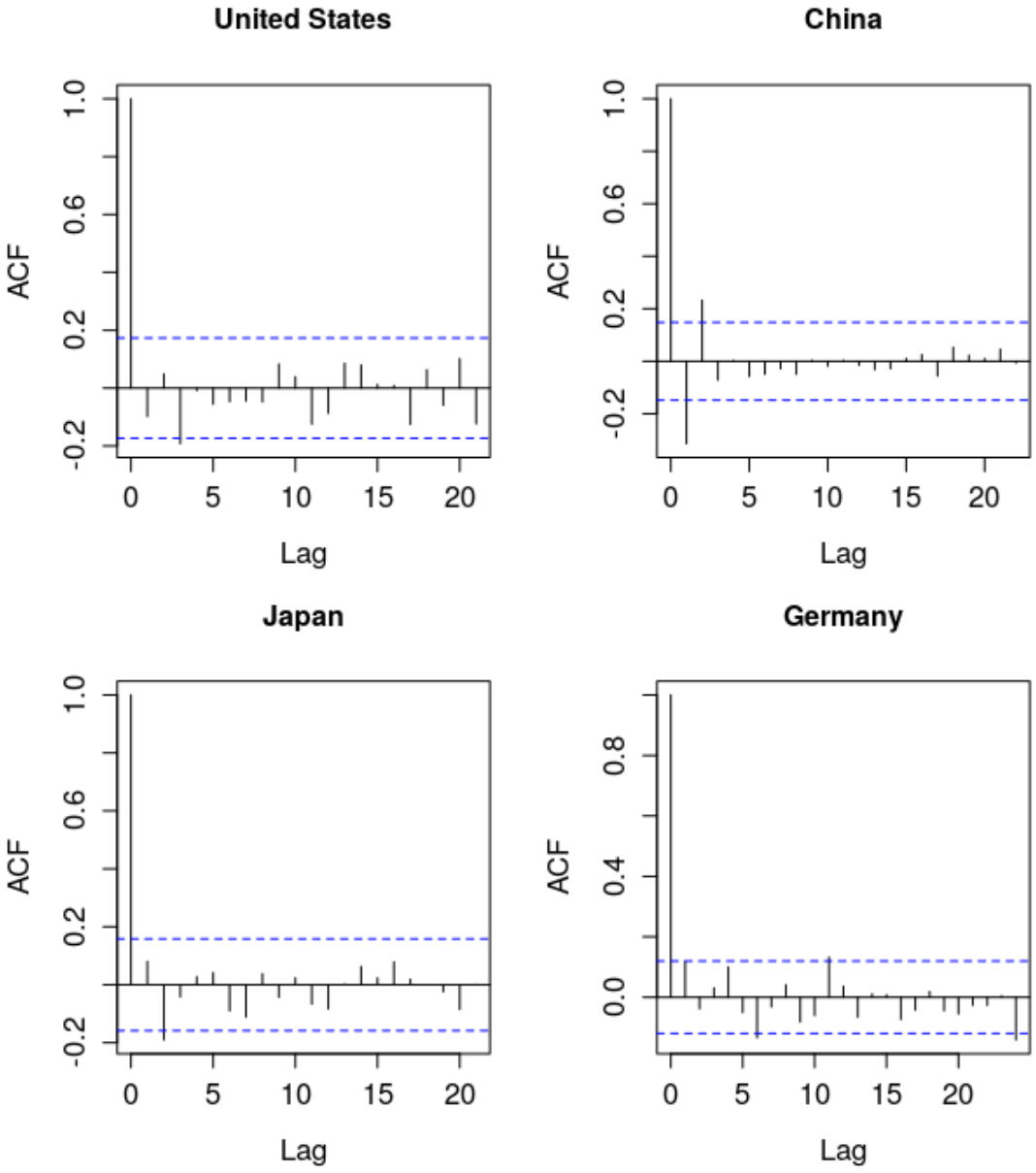

Fig. 44. Autocorrelation plots of residuals from best GNARX model. (US, China, Japan, Germany)

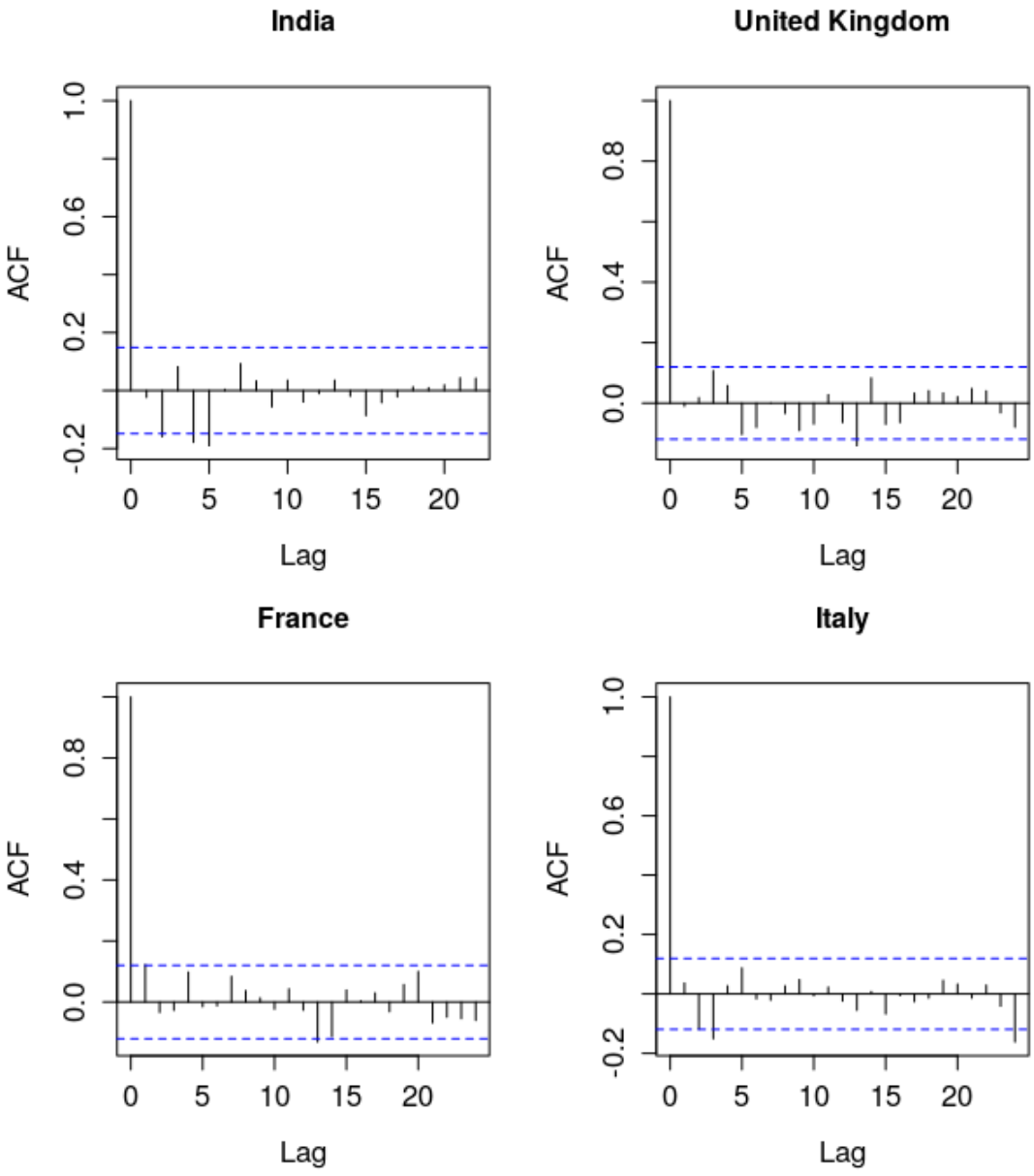

Fig. 45. Autocorrelation plots of residuals from best GNARX model. (India, UK, France, Italy)

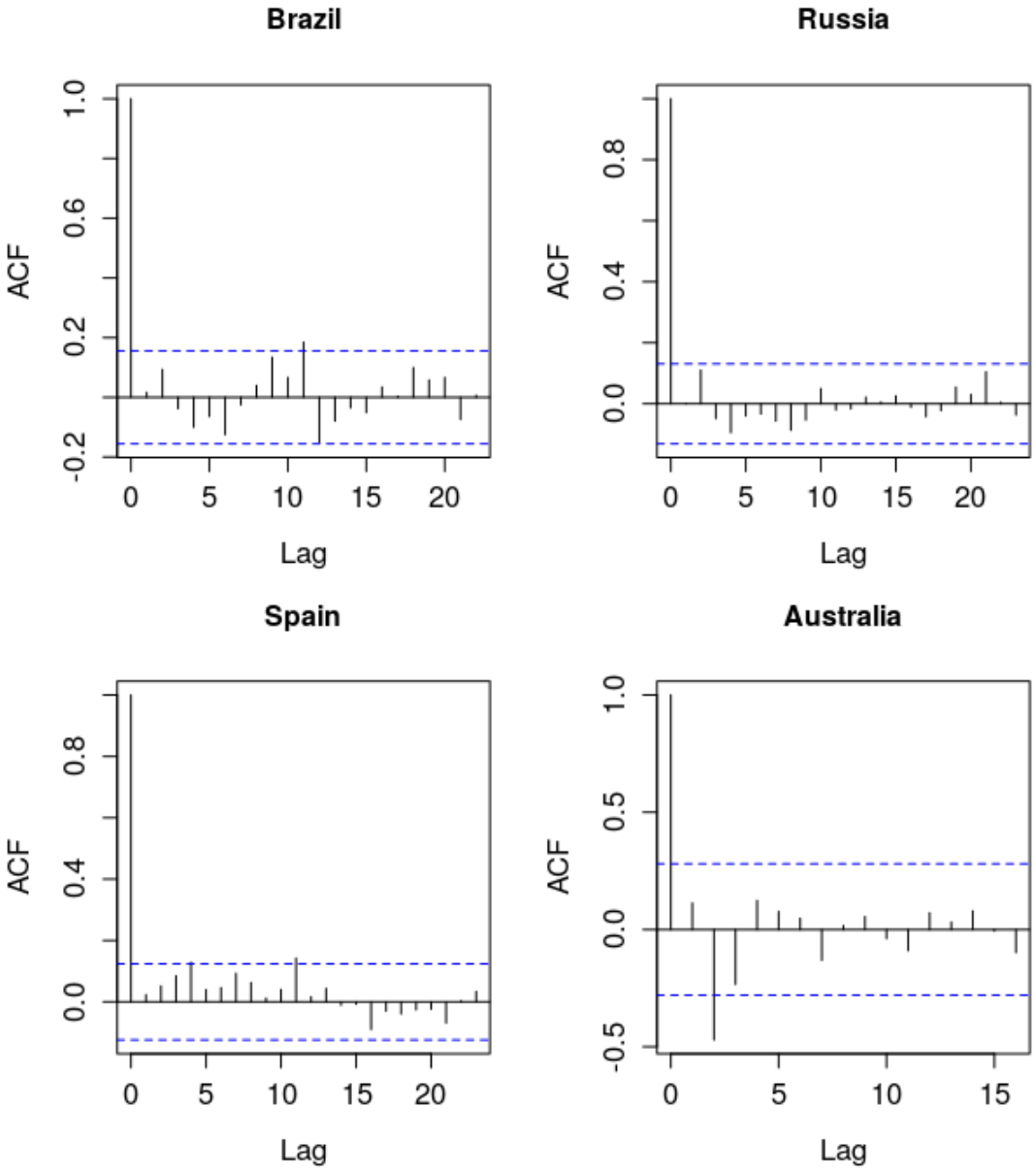

Fig. 46. Autocorrelation plots of residuals from best GNARX model. (Brazil, Russia, Spain, Australia)

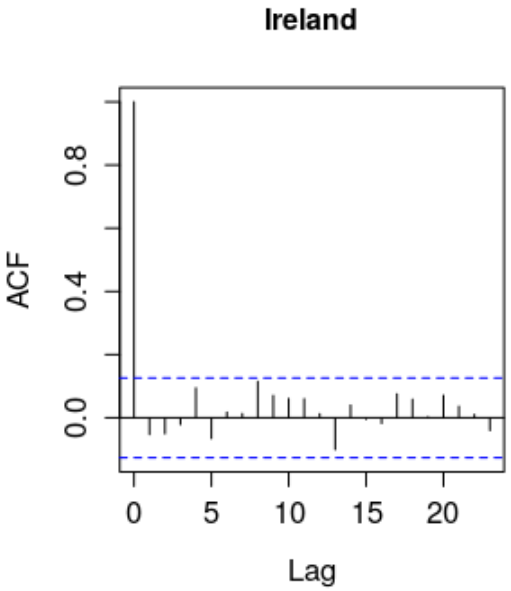

Fig. 47. Autocorrelation plots of residuals from best GNARX model. (Ireland)

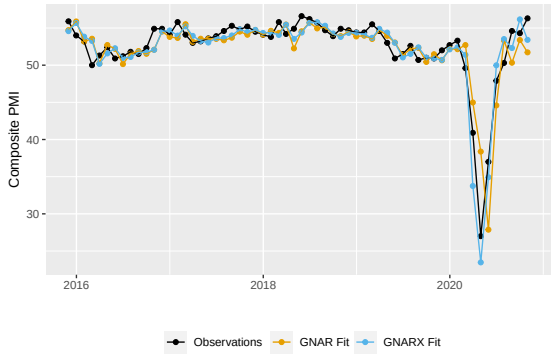

Fig. 48. United States: Comparison of GNARX$(5, [1, 0, 1, 0, 1])$ and GNARX$(5, [1, 0, 1, 0, 1], 3, 2)$ fits.

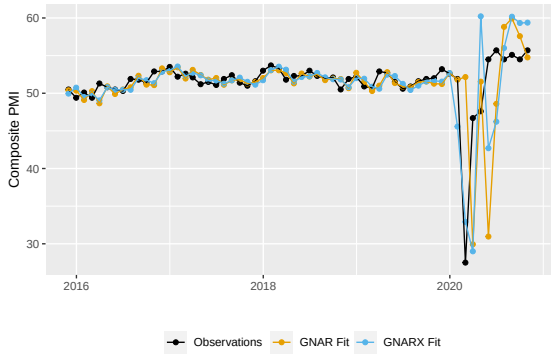

Fig. 49. China: Comparison of GNARX$(5, [1, 0, 1, 0, 1])$ and GNARX$(5, [1, 0, 1, 0, 1], 3, 2)$ fits. black

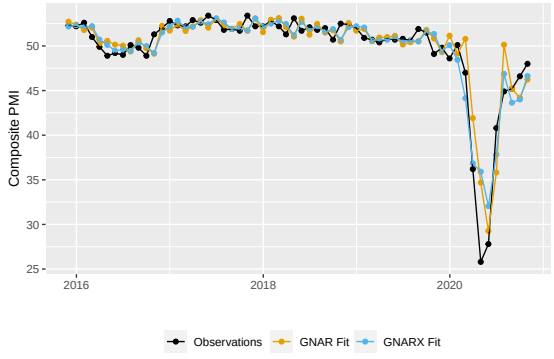

Fig. 50. Japan: Comparison of GNARX$(5, [1, 0, 1, 0, 1])$ and GNARX$(5, [1, 0, 1, 0, 1], 3, 2)$ fits.

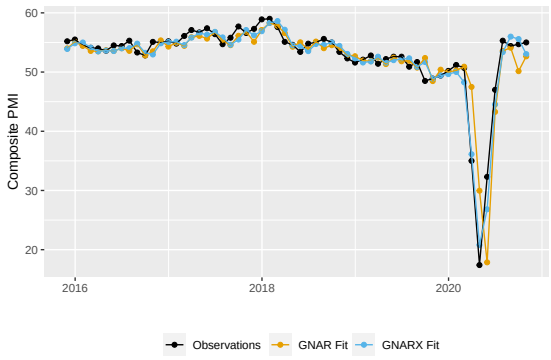

Fig. 51. Germany: Comparison of GNARX$(5, [1, 0, 1, 0, 1])$ and GNARX$(5, [1, 0, 1, 0, 1], 3, 2)$ fits.

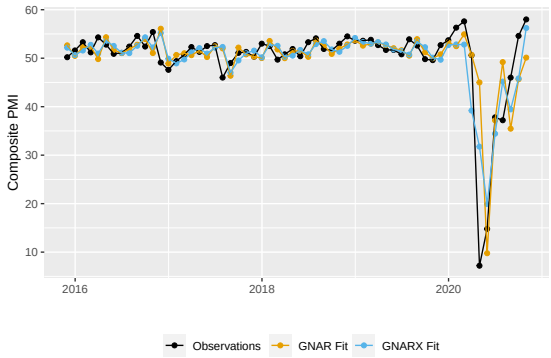

Fig. 52. India: Comparison of GNARX$(5, [1, 0, 1, 0, 1])$ and GNARX$(5, [1, 0, 1, 0, 1], 3, 2)$ fits.

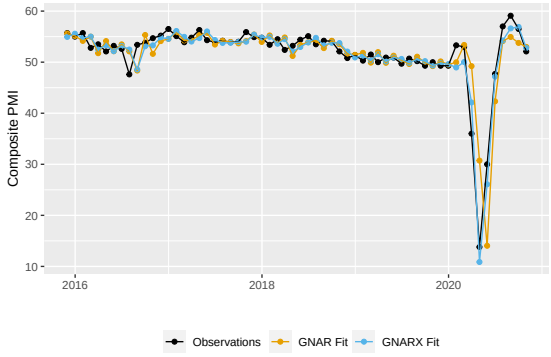

Fig. 53. United Kingdom: Comparison of GNARX$(5, [1, 0, 1, 0, 1])$ and GNARX$(5, [1, 0, 1, 0, 1], 3, 2)$ fits.

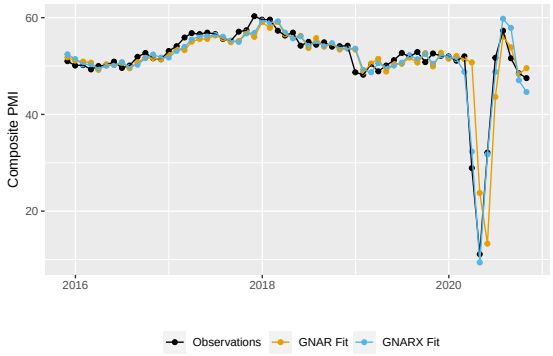

Fig. 54. France: Comparison of GNARX$(5, [1, 0, 1, 0, 1])$ and GNARX$(5, [1, 0, 1, 0, 1], 3, 2)$ fits.

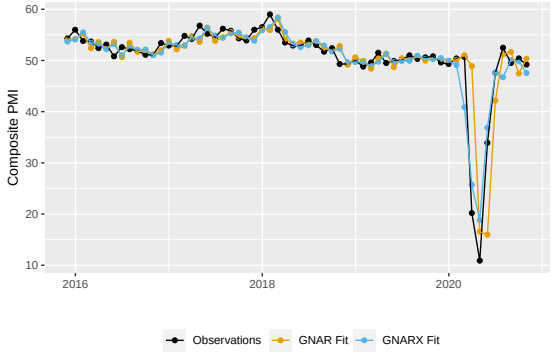

Fig. 55. Italy: Comparison of GNARX$(5, [1, 0, 1, 0, 1])$ and GNARX$(5, [1, 0, 1, 0, 1], 3, 2)$ fits.

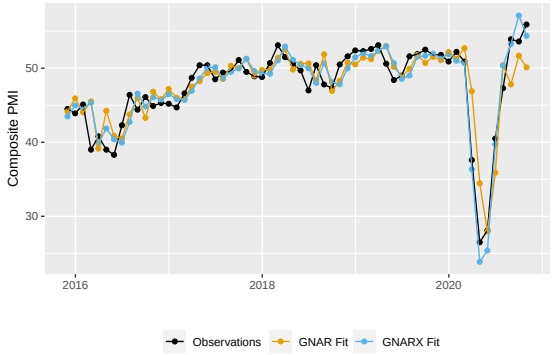

Fig. 56. Brazil: Comparison of GNARX$(5, [1, 0, 1, 0, 1])$ and GNARX$(5, [1, 0, 1, 0, 1], 3, 2)$ fits.

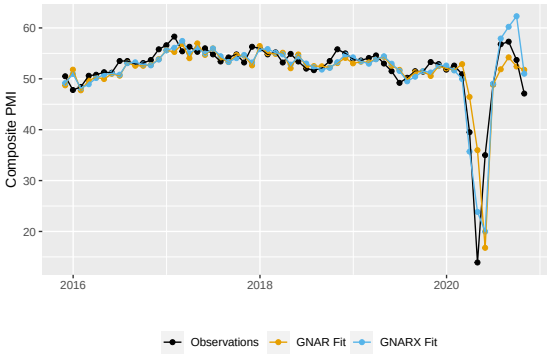

Fig. 57. Russia: Comparison of GNARX$(5, [1, 0, 1, 0, 1])$ and GNARX$(5, [1, 0, 1, 0, 1], 3, 2)$ fits.

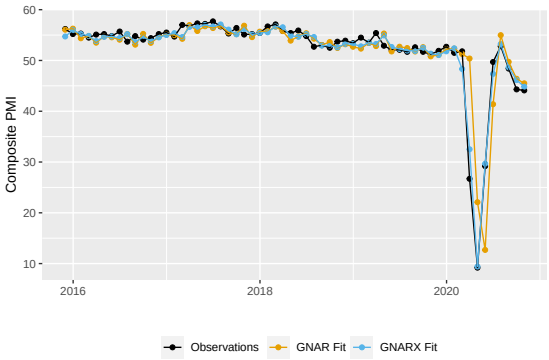

Fig. 58. Spain: Comparison of GNARX$(5, [1, 0, 1, 0, 1])$ and GNARX$(5, [1, 0, 1, 0, 1], 3, 2)$ fits.

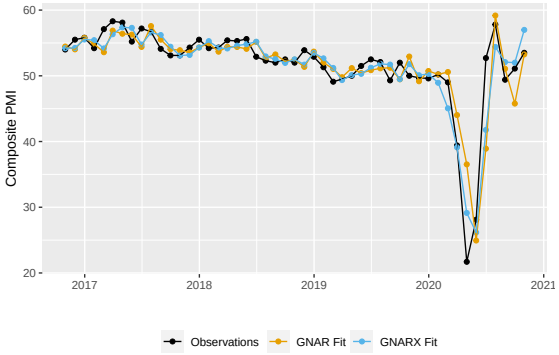

Fig. 59. Australia: Comparison of GNARX$(5, [1, 0, 1, 0, 1])$ and GNARX$(5, [1, 0, 1, 0, 1], 3, 2)$ fits.

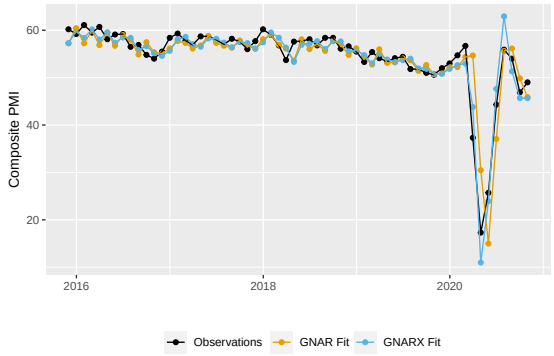

Fig. 60. Ireland: Comparison of GNARX$(5, [1, 0, 1, 0, 1])$ and GNARX$(5, [1, 0, 1, 0, 1], 3, 2)$ fits.

Table 5. In-sample composite PMI forecast performance between Jan-98 and Oct-20 using GNARX models. MSFE=In-sample mean-squared forecasting error.

Model	Model order	BIC	MSFE (SE)
Without external regressors			
Global-α GNAR, fully-connected net	4, (1, 1, 1, 0)	12653	7.1 (0.9)
Global-α GNAR, nearest-neighbour net	4, (1, 1, 1, 0)	12895	7.8 (1.0)
Local-α GNAR, fully-connected net	3, (1, 1, 1)	12806	6.7 (0.9)
Local-α GNAR, nearest-neighbour net	3, (1, 1, 1)	13036	7.4 (1.0)
AR	3	13049	7.5 (1.0)
Stringency indices only			
Global-α GNARX, fully-connected net	5, (1, 0, 1, 0, 1), 3	11323	4.2 (0.3)
Global-α GNARX, nearest-neighbour net	2, (0, 0), 3	11409	4.4 (0.4)
Local-α GNARX, fully-connected net	2, (1, 1), 3	11331	4.0 (0.3)
Local-α GNARX, nearest-neighbour net	2, (0, 0), 3	11364	4.1 (0.3)
AR	2, 3	11364	4.1 (0.3)
COVID-19 death rates only			
Global-α GNARX, fully-connected net	4, (1, 1, 1, 0), 3	12020	5.5 (0.8)
Global-α GNARX, nearest-neighbour net	4, (0, 0, 0, 0), 1	12324	6.3 (0.9)
Local-α GNARX, fully-connected net	2, (1, 1), 3	12212	5.5 (0.8)
Local-α GNARX, nearest-neighbour net	2, (0, 0), 3	12389	6.0 (0.8)
AR	2, 3	12389	6.0 (0.8)
With both external regressors			
Global-α GNARX, fully-connected net	5, (1, 0, 1, 0, 1), 3, 2	11175	4.0 (0.3)
Global-α GNARX, nearest-neighbour net	2, (0, 0), 3, 0	11301	4.2 (0.4)
Local-α GNARX, fully-connected net	2, (1, 1), 3, 1	11199	3.8 (0.3)
Local-α GNARX, nearest-neighbour net	2, (0, 0), 3, 0	11264	3.9 (0.3)
AR	2, 3, 0	11264	3.9 (0.3)

12. Generating bootstrap prediction intervals for the GNARX model

In order to obtain asymptotically pertinent prediction intervals for GNARX model forecasts, we provide a forward bootstrap algorithm similar to the algorithm used for linear autoregressive models described in Pan and Politis (2016). These prediction intervals account for both innovations in the PMI series and estimation error in the GNARX parameters, which are assumed to be independent. The pseudo-code is provided in Algorithm 1.

Algorithm 1: Generating h-step ahead bootstrap prediction intervals for the GNARX model

procedure

Input: GNARX model order $(p, \mathbf{s}, \mathbf{p}')$, observed data $\{(\mathbf{X}_{1,t}, ..., \mathbf{X}_{H,t}, \mathbf{Y}_t), t = 1, ..., T\}$, forecast steps h, and scenario assumptions for exogenous regressors $\{(\mathbf{X}_{1,t}, ..., \mathbf{X}_{H,t}), t = T+1, ..., T+h\}$, number of bootstrap samples B and prediction interval coverage $(1-\alpha)100\%$.

Output: $(1-\alpha)100\%$ prediction interval for $\mathbf{Y}_{T+h}$.

$p^* \leftarrow \max(p, p'_1, .., p'_H)$

$\hat{\gamma} \leftarrow$ GNARX parameter estimates using $\{(\mathbf{X}_{1,t}, ..., \mathbf{X}_{H,t}, \mathbf{Y}_t), t = 1, ..., T\}$

$\{\hat{\mathbf{u}}_t, t = p^* + 1, ..., T\} \leftarrow$ GNARX residuals using $\{(\mathbf{X}_{1,t}, ..., \mathbf{X}_{H,t}, \mathbf{Y}_t), t = 1, ..., T\}$

$b \leftarrow 0$

repeat

$\{\mathbf{u}^*_t, t = p^* + 1, ..., T\} \leftarrow$ samples with replacement from $\{\hat{\mathbf{u}}_t, t = p^* + 1, ..., T\}$

$(\mathbf{Y}^*_1, ..., \mathbf{Y}^*_p) \leftarrow$ sample from $\{(\mathbf{Y}_k, ..., \mathbf{Y}_{k+p^*-1}), k = 1, ..., T - p^* + 1\}$

$\{\mathbf{Y}^*_t, t = p^* + 1, ..., T\} \leftarrow$ simulations from the GNARX model with parameters $\hat{\gamma}$, starting values $(\mathbf{Y}^*_1, ..., \mathbf{Y}^*_p)$, residuals $\{\mathbf{u}^*_t, t = p^* + 1, ..., T\}$ and exogenous regressors $\{(\mathbf{X}_{1,t}, ..., \mathbf{X}_{H,t}), t = 1, ..., T\}$ (i.e. in the same order as the observed exogenous regressor time series)

$\hat{\gamma}^* \leftarrow$ GNARX parameter estimates using $\{(\mathbf{X}_{1,t}, ..., \mathbf{X}_{H,t}, \mathbf{Y}^*_t), \forall t\}$

$\left\{\hat{\mathbf{Y}}^*_{T+1}, ..., \hat{\mathbf{Y}}^*_{T+h}\right\} \leftarrow$ predicted values from the GNARX model with parameters $\hat{\gamma}^*$, data $\{(\mathbf{X}_{1,t}, ..., \mathbf{X}_{H,t}, \mathbf{Y}_t), t = 1, ..., T\}$ and scenario assumptions $\{(\mathbf{X}_{1,t}, ..., \mathbf{X}_{H,t}), t = T+1, ..., T+h\}$

$\left\{\mathbf{Y}^*_{T+1}, ..., \mathbf{Y}^*_{T+h}\right\} \leftarrow$ simulated values from the GNARX model with parameters $\hat{\gamma}$, data $\{(\mathbf{X}_{1,t}, ..., \mathbf{X}_{H,t}, \mathbf{Y}_t), t = 1, ..., T\}$, scenario assumptions $\{(\mathbf{X}_{1,t}, ..., \mathbf{X}_{H,t}), t = T+1, ..., T+h\}$ and residuals $\{\mathbf{u}^*_t, t = T+1, ..., T+h\}$

$\mathbf{e}_b \leftarrow \mathbf{Y}^*_{T+h} - \hat{\mathbf{Y}}^*_{T+h}$

$b \leftarrow b + 1$

until $b = B$;

$q(\alpha/2) \leftarrow \alpha/2$-quantile of empirical distribution of $\{\mathbf{e}_b, b = 1, .., B\}$ (i.e. an N-length vector where the i-th entry is the quantile of the empirical distribution of the i-th entry of $\mathbf{e}_b$ over all b)

$q(1-\alpha/2) \leftarrow (1-\alpha/2)$-quantile of empirical distribution of $\{\mathbf{e}_b, b = 1, .., B\}$

$\left\{\hat{\mathbf{Y}}_{T+1}, ..., \hat{\mathbf{Y}}_{T+h}\right\} \leftarrow$ predicted values from the GNARX model with parameters $\hat{\gamma}$, data $\{(\mathbf{X}_{1,t}, ..., \mathbf{X}_{H,t}, \mathbf{Y}_t), t = 1, ..., T\}$ and scenario assumptions $\{(\mathbf{X}_{1,t}, ..., \mathbf{X}_{H,t}), t = T+1, ..., T+h\}$

return $[\hat{\boldsymbol{Y}}_{T+h} + q(\alpha/2), \hat{\boldsymbol{Y}}_{T+h} + q(1-\alpha/2)]$

Supplementary Material References

Brockwell, P. J. and Davis, R. A. (1991) *Time Series: Theory and Methods*, Springer, New York.

Brockwell, P. J., Davis, R. A., and Fienberg, S. E. (1991) *Time series: theory and methods: theory and methods*, Springer Science & Business Media.

Chatfield, C. (2003) *The Analysis of Time Series: An Introduction*, Chapman and Hall/CRC, London, sixth edition.

Hamilton, J. D. (1994) *Time Series Analysis*, Princeton University Press, Princeton, New Jersey.

Knight, M., Leeming, K., Nason, G., and Nunes, M. (2020) Generalised network autoregressive processes and the GNAR package, *J. Statist. Soft.*, p. (to appear).

Knight, M. I., Nunes, M. A., and Nason, G. P. (2016) Modelling, Detrending and Decorrelation of Network Time Series, *ArXiv e-prints*, **1603.03221**.

Leeming, K. A. (2019) *New Methods in Time Series Analysis: Univariate Testing and Network Autoregression Modelling*, Ph.D. thesis, School of Mathematics, University of Bristol, Bristol, U.K.

Lütkepohl, H. (2005) *New introduction to multiple time series analysis*, Springer Science & Business Media, Berlin.

Nason, G. P. (2013) A test for second-order stationarity and approximate confidence intervals for localized autocovariances for locally stationary time series., *J. R. Statist. Soc.* B, **75**, 879–904.

Nason, G. P. (2016) *locits: Tests of stationarity and localized autocovariance*, R package version 1.7.3.

Pan, L. and Politis, D. N. (2016) Bootstrap prediction intervals for linear, nonlinear and nonparametric autoregressions, *Journal of Statistical Planning and Inference*, **177**, 1–27.

Priestley, M. B. (1983) *Spectral Analysis and Time Series*, Academic Press, London.

Zhu, X., Pan, R., Li, G., Liu, Y., and Wang, H. (2017) Network vector autoregression, *Ann. Statist.*, **45**, 1096–1123.